

# Action Hallucination in Generative Visual-Language-Action Models

Harold Soh\*† and Eugene Lim\*

\*Dept. of Computer Science, School of Computing, National University of Singapore.

†Smart Systems Institute, National University of Singapore.

Email: [harold@nus.edu.sg](mailto:harold@nus.edu.sg)

**Abstract**—Robot Foundation Models such as Vision-Language-Action models are rapidly reshaping how robot policies are trained and deployed, replacing hand-designed planners with end-to-end generative action models. While these systems demonstrate impressive generalization, it remains unclear whether they fundamentally resolve the long-standing challenges of robotics. We address this question by analyzing action hallucinations that violate physical constraints and their extension to plan-level failures. Focusing on latent-variable generative policies, we show that hallucinations often arise from structural mismatches between feasible robot behavior and common model architectures. We study three such barriers—topological, precision, and horizon—and show how they impose unavoidable tradeoffs. Our analysis provides mechanistic explanations for reported empirical failures of generative robot policies and suggests principled directions for improving reliability and trustworthiness, without abandoning their expressive power.

## I. INTRODUCTION

Robot Foundation Models (RFMs) and Large-scale Vision-Language-Action (VLA) models (e.g., [55, 24, 2, 34]) promise a “GPT moment” for robotics: given image observations and a natural-language instruction, a single end-to-end policy produces a continuous control trajectory that solves the task. Recent generative VLAs such as  $\pi_{0.5}$  [16], GrOOT N1 [34], and MolmoAct [26] combine transformer encoders with conditional flow/diffusion models that map Gaussian noise into full action trajectories. Other contenders like diffusion policies [5, 28] and flow-matching policies [51] map Gaussian noise into action chunks that are executed sequentially. These models demonstrate impressive semantic generalization, yet substantial prior work [50, 7, 46, 20, 6] has shown they also generate actions that are physically invalid, e.g., grasps through objects or plans that cannot be executed. We refer to this phenomenon as *action hallucination*.

Action hallucinations matter for two reasons. First, they are safety- and reliability-critical. Unlike hallucinated text, invalid actions are executed in the physical world and can cause damage or hazardous interactions. Second, these failures may not be confined to exotic corner cases. Even a model that is highly capable *on average* can intermittently produce nonsensical actions, a risk that is amplified when robots are deployed at scale and over long periods of time.

This paper argues that part of action hallucination is *structural*: it arises from a mismatch between (i) the geometry/topology of physically valid behavior in robotics and (ii) the architectural regularities of modern generative action heads and

planning pipelines. Concretely, many VLAs generate actions by sampling a *connected* latent prior (typically Gaussian noise) and decoding it through a map that is continuous in the latent (as in diffusion, flow-matching, and conditional flows). At execution time, these models are often used sequentially and/or wrapped in test-time sampling (and possible verification). Our goal is not to claim that these design choices are “wrong”—they can enable powerful generalization and smooth behavior—but to clarify *when* they induce hallucinations and *what* changes are needed to mitigate them.

**Contributions.** We use largely elementary mathematical tools (topology, measure bounds, and probabilistic arguments) to construct a coherent theory of action hallucination that matches the architectural and algorithmic characteristics of modern VLAs. This approach connects to classic insights in robotics and leads to a clean formal framework to analyze generative VLAs—the constraints of non-convexity, precision, and compounding errors are foundational to robotics [30, 12, 39] and our contribution is to rigorously study these constraints in the context of modern VLAs. Concretely, we contribute:

- A **topological impossibility result** for hallucination-free multi-mode coverage under continuous latent heads, and a quantitative **isoperimetric lower bound** connecting hallucination to decoder smoothness and mode separation.
- A **precision-barrier analysis** for contact tasks, including a lower bound and a **generative precision trilemma** (fold, collapse, or hallucinate), plus a refinement-step tradeoff that clarifies why iterative diffusion/flow-style generation helps.
- A reliability-aware analysis of **verification-guided planning for long-horizon tasks** that identifies when test-time compute helps, when it cannot, and why adaptive (geometrically amplifying) search is essential under verifier noise.

We also discuss connections to the growing literature of empirical results on VLAs (e.g., [2, 26, 6, 20] and to practical system design choices, e.g., hybrid discrete-continuous structure for mode selection, iterative refinement for precision, and adaptive verification-guided search for long horizons.

## II. RELATED WORK

Hallucination has been extensively studied in LLMs and VLAs (e.g., [14, 27, 45, 22]), most commonly framed as

fluent generations that violate an external correctness oracle such as factuality, groundedness, or visual consistency [19]. We adopt this oracle-based perspective, but shift the oracle from “truthfulness of text” to *physical and task validity* of actions and plans in embodied settings. In this sense, we connect hallucination-style failure modes to the feasibility structure of robot behaviors and to the design choices incorporated into modern generative action heads.

A central theme in robotics is that feasibility is rarely convex or safely “interpolatable”. Obstacles induce nonconvex and often disconnected free spaces in configuration space [30], and narrow passages can make connecting feasible components extremely hard to find [12, 13]. Contact-rich manipulation adds an additional layer of geometric fragility, where success may require reaching lower-dimensional contact sets and navigating thin mode transitions [32, 31, 29, 11]. In parallel, theory on deep generative models formalizes a related topological mismatch. With a connected latent prior and continuous generator, disconnected target supports cannot be matched exactly, leading to mode dropping or “bridging” samples [41, 23, 44, 17, 37, 43]. Here, we study these geometric and topological constraints in the context of embodied action generation.

Finally, our discussion relates to long-horizon decision-making and verification-guided search. Multi-step planning is known to be computationally challenging [38, 4] and compounding error in sequential prediction is a classic driver of long-horizon failure in imitation learning [39]. From a probabilistic viewpoint, long-horizon success can become a rare event, which motivated decomposition and adaptive sampling ideas [21, 40]. Have VLAs somehow bypassed such constraints by scaling learning and test-time compute [25, 48, 53]? Our contribution is to formalize, at a high level, how horizon-induced rarity, verifier noise, and adaptive proposal mechanisms interact to shape (and sometimes limit) the reduction of behavioral hallucinations.

### III. PRELIMINARIES

In this section, we first formalize robot environments, task instances, and robot policies. Building on this framework, we examine action (or more broadly, behavior) hallucinations for embodied AI. In LLMs, hallucinations refer to fluent outputs that violate a (possibly implicit) ground-truth oracle for factual correctness [19]. In VLAs, the output is not text but behavior: low-level actions, action chunks, or plans. As such, we define hallucinations relative to ground-truth validity oracles in a robot environment.

Given the structure of existing VLAs, we consider two major types of behavior hallucinations. At the low-level, an *action hallucination* is an action (or action chunk / trajectory) whose induced rollout violates physical laws or environmental constraints (e.g., teleporting the robot, penetrating a solid obstacle, or exceeding kinematic limits). At the high-level, even physically valid actions can still fail to achieve the task goal. Hence, a *plan hallucination* is a generated plan (sequence of actions) that violates constraints and/or fails to reach the goal. Plan hallucinations subsume action hallucinations but also

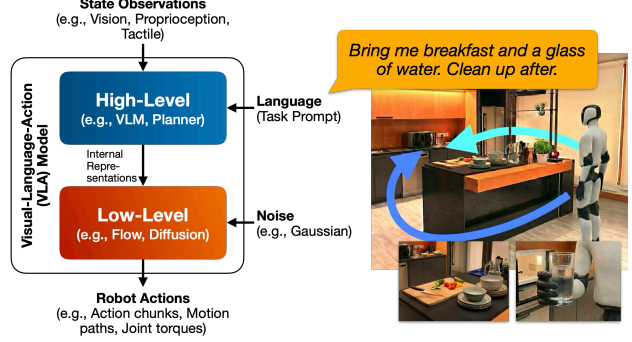


Fig. 1: (Left) The prototypical generative VLA analyzed in this work. Given state observations, a task prompt, and a noise sample, the model outputs robot actions. Recent VLAs are structured into a high-level planner and a low-level action head, but part of our theory also applies to those that do not have this explicit structure (e.g., Diffusion Policy [5], RDT [28]). (Right) An example where a robot is given a long-horizon task that involves multi-modality and precision.

include *goal failure*. Due to space constraints, we focus on the core ideas. Full proofs, formal arguments, and additional details are provided in the appendix.

#### A. Environment Model and Tasks

**Definition 1** (Environment). *An environment is a tuple*

$$\mathcal{E} = (\mathcal{S}, \mathcal{A}, \mathcal{T}, \mathcal{C}_{\text{safe}})$$

where:

- $\mathcal{S} \subseteq \mathbb{R}^n$  is the continuous state space (e.g., robot configuration and object poses, or a latent representation).
- $\mathcal{A} \subseteq \mathbb{R}^d$  is the action space (e.g., joint velocities, torques, parameterized trajectories, or action chunks).
- $\mathcal{T} : \mathcal{S} \times \mathcal{A} \rightarrow \mathcal{S}$  is a deterministic transition map
- $\mathcal{C}_{\text{safe}} \subseteq \mathcal{S}$  is the “safe” set of physically-consistent and constraint-satisfying states.

We deliberately keep this model simple. It turns out that hallucinations will already occur in this simplified setting, and our statements can be extended to encompass stochasticity and partial observability. We consider the common setting that the robot is tasked to achieve a particular goal.

**Definition 2** (Goal-Reaching Task Instance). *A task instance is a tuple*

$$I = (\mathcal{E}, s_0, \mathcal{G}, T)$$

where  $\mathcal{E}$  is an environment,  $s_0 \in \mathcal{C}_{\text{safe}}$  is an initial state,  $\mathcal{G} \subseteq \mathcal{C}_{\text{safe}}$  is a goal set, and  $T \in \mathbb{N}$  is a horizon (time or action-budget).

#### B. Robot Policies with Latent Generative Heads

Many modern VLAs use a *latent-variable* generative head (diffusion, flow matching) to produce continuous actions or action chunks (Fig. 1). They are typically invoked in a closed-loop manner; the model generates an action, the robot executes it, new observations arrive, and the model is queried again.

**Assumption 3** (Latent Prior). *The latent space  $\mathcal{Z}$  is a nonempty, open, and path-connected subset of  $\mathbb{R}^m$ . The latent prior  $p_Z$*

is a probability measure on  $\mathcal{Z}$  that is absolutely continuous with respect to  $m$ -dimensional Lebesgue measure, and has a density  $\rho_Z$  such that  $\rho_Z(z) > 0$  for almost every  $z \in \mathcal{Z}$ . Moreover, for every compact set  $K \subset \mathcal{Z}$ , there exists a constant  $\rho_{\min}(K) > 0$  such that  $\rho_Z(z) \geq \rho_{\min}(K)$  for almost every  $z \in K$ . We further assume that the dimensionality of the latent code  $z$  is the same as the action,  $m = d$  (as the case in flow-matching and diffusion models).

**Definition 4** (Latent-Head Policy). *Let Assumption 3 hold. A latent-head policy is a map parameterized by  $\theta$ ,  $\pi_\theta : \mathcal{S} \times \mathcal{Z} \rightarrow \mathcal{A}$ , that is defined for every  $(s, z)$  (i.e., total). We assume:*

- 1) Continuity in the latent: for each fixed  $s \in \mathcal{S}$ , the map  $z \mapsto \pi_\theta(s, z)$  is continuous on  $\mathcal{Z}$ .
- 2) Finite computation: there exists a polynomial  $q$  such that for any  $(s, z)$ ,  $\pi_\theta(s, z)$  can be computed in time at most  $q(|s| + |z|)$ .

The action distribution induced by  $\pi_\theta$  at state  $s$  is  $a \sim p_\theta(\cdot | s) := (\pi_\theta(s, \cdot)) \# p_Z$ .

The abstraction above captures both low-level diffusion/flow-based policies and more complex VLA policies with transformer encoders and continuous flow-matching heads. In typical models, the latent  $z$  is Gaussian noise, the head  $\pi_\theta(s, \cdot)$  is continuous in  $z$ , and the overall computation is bounded by a fixed-depth network along with a finite number of ODE integration steps. During execution, the robot policy is typically deployed in a closed-loop fashion. Definition 5 below lets us discuss planning behavior even when a VLA does not emit a full plan upfront since a closed-loop controller still induces a finite action sequence when unrolled.

**Definition 5** (Closed-Loop Rollout and Induced Plan). *Fix a horizon  $T \in \mathbb{N}$ . Given an initial state  $s_0 \in \mathcal{S}$  and a latent sequence  $z_{0:T-1} = (z_0, \dots, z_{T-1}) \in \mathcal{Z}^T$ , define the closed-loop rollout recursively by  $a_t = \pi_\theta(s_t, z_t)$ ,  $s_{t+1} = \mathcal{T}(s_t, a_t)$  for  $t = 0, \dots, T-1$ . The resulting action sequence*

$$\tau_\theta(s_0, z_{0:T-1}) := (a_0, \dots, a_{T-1}) \in \mathcal{A}^T$$

is the induced plan produced by the closed-loop policy over horizon  $T$ . At deployment, one typically samples fresh  $Z_t \sim p_Z$  at each step, so  $\tau_\theta(s_0, Z_{0:T-1})$  is a random variable induced by the policy and the environment.

### C. Behavior Hallucinations: Action and Plan

In LLMs, hallucinations refer to fluent outputs that violate a (possibly implicit) ground-truth oracle for factual correctness [19]. In VLAs, the output is not text but behavior: low-level actions, action chunks, or possibly long-horizon plans. As such, we consider behavior hallucinations relative to ground-truth validity oracles in a robot environment.

**Definition 6** (Physical Validity Oracle). *For a fixed environment  $\mathcal{E}$ , define the one-step physical validity predicate  $f_{\text{phys}} : \mathcal{S} \times$*

$\mathcal{A} \rightarrow \{0, 1\}$  where

$$f_{\text{phys}}(s, a) = \begin{cases} 1 & \text{if the rollout induced by } (s, a) \\ & \text{stays in } \mathcal{C}_{\text{safe}}, \\ 0 & \text{otherwise.} \end{cases}$$

Here the action  $a$  may denote an instantaneous control, a parameterized motion primitive, or an action chunk. In the latter cases, the predicate checks safety for all intermediate states along execution, and  $\mathcal{T}(s, a)$  denotes the terminal state after the chunk completes.

We define action hallucination as physical invalidity under  $f_{\text{phys}}$ , which can then be extended to plan hallucinations. To reduce clutter, we implicitly fold state-dependent action admissibility (e.g., torque limits, contact modes) into  $f_{\text{phys}}$ . When an action is physically impossible, we treat the corresponding transition as leaving  $\mathcal{C}_{\text{safe}}$ .

**Definition 7** (Action Hallucination). *Given an environment  $\mathcal{E}$ , state  $s \in \mathcal{S}$ , and latent  $z \in \mathcal{Z}$ , the action  $a = \pi_\theta(s, z)$  is an action hallucination at  $s$  if  $f_{\text{phys}}(s, a) = 0$ . The hallucination probability at  $s$  is*

$$H_\theta(s) := \Pr_{z \sim p_Z} [f_{\text{phys}}(s, \pi_\theta(s, z)) = 0].$$

We say the policy is hallucination-free at  $s$  if  $H_\theta(s) = 0$ .

**Definition 8** (Plan Hallucination). *Fix an instance  $I = (\mathcal{E}, s_0, \mathcal{G}, T)$ . Given an open-loop plan  $\tau = (a_0, \dots, a_{T-1}) \in \mathcal{A}^T$  and its rollout  $s_{t+1} = \mathcal{T}(s_t, a_t)$  from  $s_0$  for  $t = 0, \dots, T-1$ , we define the plan-validity predicate*

$$f_{\text{plan}}(s_0, \tau) = 1$$

if and only if (i) every executed step is physically valid, i.e.,  $f_{\text{phys}}(s_t, a_t) = 1$  for all  $t = 0, \dots, T-1$ , and (ii) the terminal state satisfies  $s_T \in \mathcal{G}$ . Otherwise set  $f_{\text{plan}}(s_0, \tau) = 0$ . A plan hallucination occurs when  $f_{\text{plan}}(s_0, \tau) = 0$ .

If a latent-head policy is deployed in closed-loop and induces the random plan  $\tau_\theta(s_0, Z_{0:T-1})$  from Definition 5, then its plan-hallucination probability on  $I$  is

$$H_\theta^{\text{plan}}(I) := \Pr_{Z_{0:T-1} \sim p_Z^{\otimes T}} [f_{\text{plan}}(s_0, \tau_\theta(s_0, Z_{0:T-1})) = 0].$$

We call  $I$  solvable if there exists a plan  $\tau \in \mathcal{A}^T$  with  $f_{\text{plan}}(s_0, \tau) = 1$ , and unsolvable otherwise.

In many VLAs, “plans” are realized as (possibly implicit) subtask sequences, skills, or waypoints. Our plan hallucination definition encompasses situations where these generated plans are not grounded in the environment or don’t compose toward the goal. We focus on hallucinations in solvable instances, so hallucination is not conflated with impossibility.

## IV. LOW-LEVEL ACTION HALLUCINATIONS

Given the above, we discuss action hallucinations that arise due to multi-modality and precision requirements in robotics.

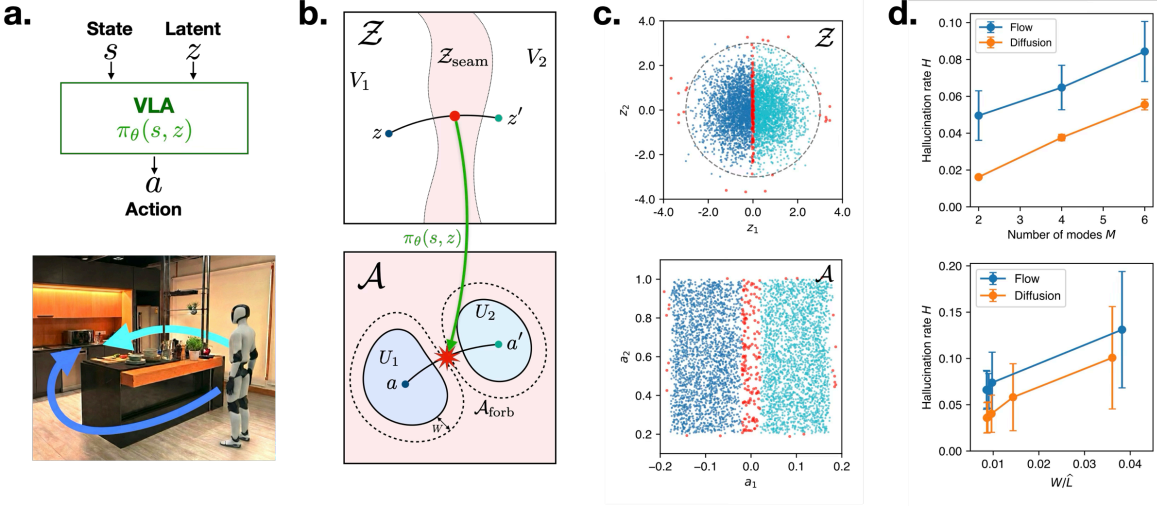


**Fig. 2: Topological barrier for latent-variable VLA policies.** (a) We study generative VLAs whose action head is a conditional latent-variable policy  $\pi_\theta(s, z)$  that maps a state (e.g., an image–language context) and latent noise  $z$  to a continuous action (or action chunk). In the illustrated navigation example, reaching the microwave requires going *left* or *right* around the kitchen island, inducing two qualitatively distinct modes of valid behaviors. (b) Schematic of the topological barrier (Lemma 10). The valid actions (bottom panel) decompose into disconnected components  $U_1$  and  $U_2$  (e.g., left vs. right), separated by a forbidden region  $\mathcal{A}_{\text{forb}}$ . If  $\pi_\theta(s, \cdot)$  is continuous and maps  $z \mapsto a \in U_1$  and  $z' \mapsto a' \in U_2$ , then any continuous latent path between  $z$  and  $z'$  must cross an *open seam*  $\mathcal{Z}_{\text{seam}} = \pi_\theta(s, \cdot)^{-1}(\mathcal{A}_{\text{forb}})$ , implying non-zero hallucination probability. Our lower bound scales with the number of modes and with  $W/L$  (a gap-smoothness ratio). (c) Diffusion model trained on bimodal action data: red points in  $\mathcal{Z}$  (top) lie on the seam and decode to forbidden actions in  $\mathcal{A}$  (bottom). See Appendix D-A for details. (d) Empirical trends for flow matching and diffusion. Hallucination rates  $H$  increases approximately linearly with the number of modes  $M$  (top) and grows with  $W/\hat{L}$  (bottom), consistent with Theorem 12 ( $\hat{L}$  is the numerically-estimated Lipschitz constant).

### A. Topological Barrier for Multi-Mode Coverage

Recent VLAs and generative policies (e.g., Diffusion Policy [5] and Flow Policy [51]) are often lauded for their ability to represent complex *multi-modal* action trajectories (e.g., “go left” or “go right” around an obstacle). However, experiments show these models still produce invalid actions despite significant training [50, 7, 20]. In this section, we first show that generative action heads cannot cover multiple disconnected safe modes without action hallucination. We then derive a more precise lower-bound using the Gaussian isoperimetric inequality that shows that smoother policies result in larger hallucination probabilities. Figure 2 provides a high-level overview.

Let us fix a state  $s \in \mathcal{S}$  and define the state-dependent safe (or valid) action set,  $\mathcal{A}_{\text{safe}}(s) := \{a \in \mathcal{A} : f_{\text{phys}}(s, a) = 1\}$ . The forbidden action set is  $\mathcal{A}_{\text{forb}}(s) := \mathcal{A} \setminus \mathcal{A}_{\text{safe}}(s)$ . We first consider situations where the valid actions at a fixed state decompose into two distinct safe ‘modes’,  $U_L$  and  $U_R$  (e.g., two inverse-kinematics branches, two grasp approach directions), separated by actions that are physically forbidden (e.g., collision, joint-limit violation, infeasible contact).

**Assumption 9** (Disconnected Safe Actions and Open Forbidden Zone). *For a given state  $s$ , assume:*

- 1) *The safe action set  $\mathcal{A}_{\text{safe}}(s)$  has at least two disjoint, nonempty path-connected components  $U_L$  and  $U_R$  in the subspace topology of  $\mathcal{A}$ .*
- 2) *The forbidden region  $\mathcal{A}_{\text{forb}}(s)$  is open in  $\mathcal{A}$  and has nonempty interior.*

*Note that the above implies that for any continuous path  $\gamma$ :*

$[0, 1] \rightarrow \mathcal{A}$  with  $\gamma(0) \in U_L$  and  $\gamma(1) \in U_R$ , there exists  $t^* \in (0, 1)$  such that  $\gamma(t^*) \in \mathcal{A}_{\text{forb}}(s)$ .

In this setting, topology dictates that a latent action head that attempts to cover both modes must hallucinate.

**Lemma 10** (Topological Barrier). *Suppose Assumption 9 holds and there exist  $z_L, z_R \in \mathcal{Z}$  such that  $\pi_\theta(s, z_L) \in U_L$  and  $\pi_\theta(s, z_R) \in U_R$ . Define the seam set,  $\mathcal{Z}_{\text{seam}}(s) := \{z \in \mathcal{Z} : \pi_\theta(s, z) \in \mathcal{A}_{\text{forb}}(s)\}$ . Then  $\mathcal{Z}_{\text{seam}}(s)$  is nonempty and open in  $\mathcal{Z}$ . The hallucination probability at  $s$  is strictly positive:*

$$H_\theta(s) = \Pr_{z \sim p_Z} [z \in \mathcal{Z}_{\text{seam}}(s)] > 0.$$

*In other words, no continuous latent-to-action map that covers both safe modes can be hallucination-free at  $s$ .*

Lemma 10 (proof in Appendix A-A) translates a known geometric concept in deep generative modeling (e.g., [23, 44, 41]) to robotics—if there are distinct modes of valid behaviors at a given state, then any generative policy that is smooth in its latent input must create a “seam” of *in-between* latents that decode to *in-between* actions. The policy cannot assign probability mass to both modes without also assigning probability mass to the invalid or unsafe actions between them. Note that Lemma 10 establishes only that the hallucination probability is non-zero; it does not quantify its magnitude nor identify factors driving hallucinations.

Next, we derive a quantitative lower bound in a multi-mode setting ( $\geq 2$ ). Assumption 11 below extends the previous setup to one where the valid action set  $\mathcal{A}_{\text{safe}}(s)$  splits into  $M$

disconnected modes  $U_1, U_2, \dots, U_M$ . These modes in action space are separated by at least a distance  $2W$  with a forbidden buffer of thickness  $W$  around each mode.

**Assumption 11** (Buffered separated modes). *For a given state  $s$ , we assume that:*

- 1) (Disconnected modes) *The safe set decomposes into  $M \geq 2$  nonempty, pairwise-disjoint, path-connected components  $\mathcal{A}_{\text{safe}}(s) = \bigsqcup_{i=1}^M U_i$ .*
- 2) (Separation by a forbidden margin) *There exists  $W > 0$  such that  $\text{dist}(U_i, U_j) := \inf_{a \in U_i, a' \in U_j} \|a - a'\| \geq 2W$  for all  $i \neq j$ , and for each  $i$  the  $W$ -neighborhood of  $U_i$  outside  $U_i$  itself is forbidden:  $\{a \in \mathcal{A} : 0 < \text{dist}(a, U_i) < W\} \subseteq \mathcal{A}_{\text{forb}}(s)$ .*

In the common Gaussian latent setting, we can lower-bound the hallucination rate of smooth policies that are locally Lipschitz in  $z$  (i.e., small changes in the latent  $z$  within a typical region cannot cause arbitrarily large jumps in action).

**Theorem 12** (Isoperimetric lower bound on action hallucination). *Fix a state  $s$  satisfying Assumption 11. Let  $Z \sim \mathcal{N}(0, I_d)$  and fix a radius  $R > 0$ . Assume that the latent-to-action head  $z \mapsto \pi_\theta(s, z)$  is  $L$ -Lipschitz on the typical-latent ball  $B_R := \{z \in \mathbb{R}^d : \|z\| \leq R\}$ , i.e.,  $\|\pi_\theta(s, z) - \pi_\theta(s, z')\| \leq L \|z - z'\| \forall z, z' \in B_R$ . Let  $\epsilon := W/L$ .*

*For each safe mode  $U_i$ , define the latent preimage  $V_i := \pi_\theta(s, \cdot)^{-1}(U_i)$  and the in-ball mass  $p_i^{(R)} := \Pr[Z \in V_i \cap B_R]$ . Let  $q(R) = \Pr[\|Z\| > R]$ . Then the hallucination probability at  $s$  satisfies*

$$H_\theta(s) \geq \sum_{i=1}^M \left[ \Phi\left(\Phi^{-1}(p_i^{(R)}) + \epsilon\right) - p_i^{(R)} \right] - q(R), \quad (1)$$

*where  $\Phi$  is the CDF of the standard normal distribution.*

Compared to Lemma 10, Theorem 12 provides a quantitative lower bound that reveals key factors that influence the action hallucination rate. As before, the problem is interpolation between the  $M$  modes. The more smoothly the policy varies with the latent, the more probability mass leaks into the forbidden seam. In addition to the number of modes  $M$ , a key ratio to note is  $\epsilon = W/L$ .  $W$  measures how wide the unsafe gap is in action space, and  $L$  measures how quickly actions can change as we adjust the latent  $z$ . If the model is very smooth in the latent space (low Lipschitz constant  $L$  within the ball  $B_R$ ), then it must transition gradually, and a larger set of latents produce intermediate invalid actions. The main idea underlying the proof (Appendix A-B) is to apply Gaussian isoperimetry to lower bound the mass of disjoint latent “halos” of radius  $\epsilon = W/L$  around each safe-mode set.

**Implications for VLAs.** Lemma 10 shows that hallucination is unavoidable for typical continuous generative policies in multi-modal environments. Theorem 12 further reveals a fundamental “mode capacity limit” for these policies. It shows that a smooth decoder can only support a finite number of distinct behaviors (modes) before the “seams” between them—the regions of hallucination—become dominant. Our

analysis reveals a persistent tension between *diversity* and *safety*. Datasets are typically multi-modal (e.g., distinct grasp types or approach trajectories) and a low-level continuous policy trained to cover all  $M$  modes faces a geometric dilemma:

- 1) **Accept Hallucination:** To cover all diverse modes, the policy is geometrically required to expose significant Gaussian surface area to the forbidden regions, which leads to invalid “interpolated” actions.
- 2) **Suffer Mode Collapse:** To reduce the hallucination rate (minimize  $H_\theta$ ), the policy can drop modes (reduce  $M$ ).

Crucially, this dilemma is a geometric consequence and not just an optimization or data problem. A theoretical solution is to break the continuity assumption: generative action heads can employ *hybrid* designs that use discrete decisions to switch between modes (e.g., discrete skill tokens [1, 15], diffusion options [8], or mixture-of-experts gating [10]). In VLAs with high-level structure, the planner can sample the mode as part of its internal representation before invoking the generative action head. However, this shifts the burden of hallucination avoidance to the high-level planner (see Sec. V).

Theorem 12 also indicates that smoothness is a “double-edged sword” for contemporary models: on one hand, smoothness is generally encouraged in (learnt) policies as it is associated with more stable training [41] and robot behavior—we usually prefer the case that similar  $z$  imply similar actions. On the other hand, smoothness likely has a *negative* effect on action hallucination; all else being equal, in (1), each term  $\Phi(\Phi^{-1}(p_i^{(R)}) + \epsilon) - p_i^{(R)}$  is increasing in  $\epsilon = W/L$ .

## B. Precision Barrier for Contact Tasks

Let us now shift our attention from multiple modes to the complementary regime of precision and contact-rich tasks. Once contact occurs, rigid-body non-penetration, admissible contact modes, and practical limits such as maximum contact wrench induce additional state-dependent constraints on which actions are physically allowed. The set of admissible actions form a thin tube around a lower-dimensional set in action space. Here, we revisit this *precision-barrier* from classical robotics [13] and we show that, as tolerance around the tube shrinks, any policy with a *smooth, full-dimensional* action density is almost guaranteed to hallucinate actions (See Fig. 3 for an overview).

We model ideal contact configurations as a state-dependent  $k$ -dimensional embedded submanifold  $\mathcal{M}(s)$ :

**Definition 13** (Contact/Precision Manifold and Tolerance). *Let  $\mathcal{M}(s) \subset \mathcal{A}$  be a compact  $C^1$  submanifold of dimension  $k < d$ . For  $\delta > 0$ , define the  $\delta$ -tube around  $\mathcal{M}(s)$  by*

$$\mathcal{M}_\delta(s) := \{a \in \mathcal{A} : \text{dist}(a, \mathcal{M}(s)) \leq \delta\},$$

*where  $\text{dist}(a, \mathcal{M}) = \inf_{x \in \mathcal{M}} \|a - x\|$ . For a state  $s$ , suppose the safe terminal actions satisfy  $\mathcal{A}_{\text{safe}}(s; \delta) \subseteq \mathcal{M}_\delta(s)$  for a task-specific tolerance  $\delta$ . Define the  $\delta$ -tolerant success  $S_\theta(s; \delta) := \Pr[a \in \mathcal{A}_{\text{safe}}(s; \delta)]$ , and hallucination probabilities,*

$$H_\theta(s; \delta) := \Pr[a \notin \mathcal{A}_{\text{safe}}(s; \delta)] = 1 - S_\theta(s; \delta).$$

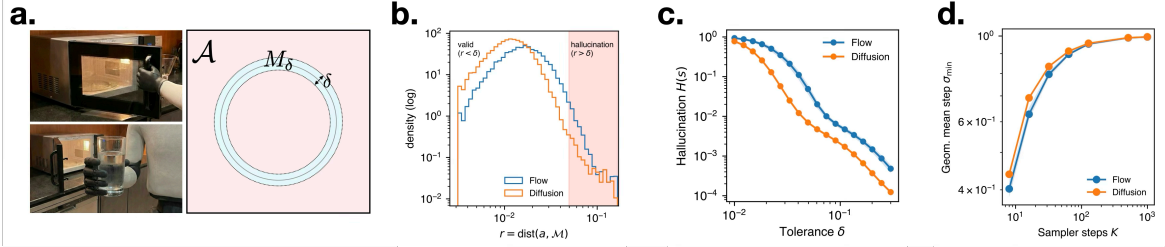


**Fig. 3: Precision barrier for contact-rich tasks.** (a) Many manipulation tasks (e.g., grasping, peg-in-hold, handling tools / articulated / deformable objects) require high precision in that valid actions concentrate near a lower-dimensional feasible set. We model this as a  $k$ -dimensional manifold  $\mathcal{M} \subset \mathcal{A}$  with tolerance tube  $\mathcal{M}_\delta = \{a : \text{dist}(a, \mathcal{M}) \leq \delta\}$  (schematic). (b) Empirical distribution of distances  $r = \text{dist}(a, \mathcal{M})$  for samples from flow matching and diffusion (log scales). The shaded region  $r > \delta$  corresponds to action hallucinations. See Appendix D-B for experiment details. (c) Action hallucination rate  $H(s; \delta) = \Pr[r > \delta]$  versus tolerance  $\delta$  (log-log). Tightening tolerance sharply increases hallucinations, consistent with our precision barrier (Lemma 14) that shows maintaining low hallucination at small  $\delta$  requires increasingly concentrated mass near  $\mathcal{M}$ . (d) The geometric mean of per-step minimum singular values,  $(\prod_{t=1}^K \sigma_{\min}(J\Phi_t))^{1/K}$ , increases toward 1 as the number of sampler steps  $K$  grows, indicating that the necessary overall contraction can be distributed across many mild refinement steps rather than a single severe collapse (Theorem 15 and Corollary 16).

We fix a state  $s$  and write  $\mathcal{M} := \mathcal{M}(s)$  and  $\mathcal{M}_\delta := \mathcal{M}_\delta(s)$  to reduce notation clutter. Recall that  $Z \sim p_Z$  satisfies Assumption 3, so  $p_Z$  has a density  $\rho_Z$  that is strictly positive and bounded on compact subsets of  $\mathcal{Z}$ . Next, we establish that hitting a low-dimensional contact manifold requires the action distribution to concentrate its probability density.

**Lemma 14** (Precision Barrier). *Fix a state  $s$  and adopt Definition 13. Then, there exist constants  $C_{\mathcal{M}} > 0$  and  $\bar{\delta} > 0$  (depending only on  $\mathcal{M}$ ) such that for all  $0 < \delta \leq \bar{\delta}$ ,  $H_\theta(s; \delta) \leq C_{\mathcal{M}} \delta^{d-k} \cdot \text{ess sup}_{a \in \mathcal{M}_\delta} p(a \mid s)$ , and hence*

$$H_\theta(s; \delta) \geq 1 - C_{\mathcal{M}} \delta^{d-k} \cdot \text{ess sup}_{a \in \mathcal{M}_\delta} p(a \mid s). \quad (2)$$

If  $H_\theta(s; \delta) \leq \eta$  for some  $\eta \in (0, 1)$ , then  $\text{ess sup}_{a \in \mathcal{M}_\delta} p(a \mid s) \geq \frac{1-\eta}{C_{\mathcal{M}}} \delta^{-(d-k)}$ .

Lemma 14 (proof in Appendix B-A) captures a source of action hallucination that is *distinct* from the topological barrier in Section IV-A. Even when the valid action set is connected (a single contact manifold), the policy needs to generate probability densities scaling as  $O(\delta^{-(d-k)})$  inside the  $\delta$ -tube around  $\mathcal{M}$ . This becomes more challenging as the tolerance  $\delta$  shrinks or the codimension ( $d - k$ ) increases. The following theorem shows how a policy can supply this extreme density.

**Theorem 15** (The Precision Trilemma: Collapse, Fold, or Hallucinate). *Let the action be generated by  $a = F(z)$  where  $Z \sim p_Z$ . Assume  $F$  is  $C^1$  on an open set  $U \subseteq \mathcal{Z}$  containing the support of  $p_Z$ , with bounded latent density  $\rho_Z(z) \leq \rho_Z^{\max}$ . Define the active latent set as  $Z_\delta := F^{-1}(\mathcal{M}_\delta) \cap U$ . Define local folding and local conditioning restricted to this active set:  $N_\delta := \text{ess sup}_{a \in \mathcal{M}_\delta} \#\{z \in Z_\delta : F(z) = a\}$ , and  $\sigma_*(\delta) := \text{ess inf}_{z \in Z_\delta} \sigma_{\min}(J_F(z))$ , where  $J_F(z)$  is the Jacobian of  $F$  and  $\sigma_{\min}(J_F(z))$  its smallest singular value. Assume  $F$  is finite-to-one on  $Z_\delta$  (i.e.,  $N_\delta < \infty$ ) and  $\sigma_*(\delta) > 0$ . Then the induced action distribution admits a density on  $\mathcal{M}_\delta$  and the hallucination rate satisfies*

$$H_\theta(s; \delta) \geq 1 - C_{\mathcal{M}} \delta^{d-k} N_\delta \rho_Z^{\max} \sigma_*(\delta)^{-d}. \quad (3)$$

In particular, if the policy achieves a target hallucination level  $H_\theta(s; \delta) \leq \eta$  for some  $\eta \in (0, 1)$ , then the generator must satisfy the following lower bound locally on the tube:

$$\underbrace{N_\delta \cdot \sigma_*(\delta)^{-d}}_{\text{Fold}} \geq \underbrace{\frac{1-\eta}{C_{\mathcal{M}} \rho_Z^{\max}}}_{\text{Collapse}} \delta^{-(d-k)}. \quad (4)$$

Hence, as precision tightens ( $\delta \rightarrow 0$ ), any policy that maintains  $H_\theta(s; \delta) \leq \eta$  must either fold space ( $N_\delta \rightarrow \infty$ ) or collapse volume locally ( $\sigma_*(\delta) \rightarrow 0$ ).

Theorem 15 (proof in Appendix B-B) shows that near the tube, the induced action density satisfies  $p(a \mid s) \lesssim N_\delta \cdot \rho_Z^{\max} \cdot \sigma_*(\delta)^{-d}$  so the two architectural mechanisms to increase density are:

- 1) Collapse (Jacobian contraction): make  $\sigma_*(\delta)$  small so  $F$  compresses latent volume into a tiny region of action space.
- 2) Fold (many-to-one decoding): make  $N_\delta$  large so that many disjoint latent regions decode to the same actions.

If neither occurs, the policy cannot place enough mass in the tube and will hallucinate actions. In short, as  $\delta \rightarrow 0$ , the generative policy must either collapse, fold, or hallucinate.

Modern VLAs (as in Fig. 1) typically use flow-matching or DDIM to generate actions. These are diffeomorphic generators so folding is not possible ( $N_\delta = 1$ ) and meeting the density requirement at tight tolerances *requires* Jacobian collapse. These methods apply a sequence of “refinement” (or denoising) steps and Corollary 16 below (proof in Appendix B-C) shows that to maintain a fixed hallucination rate at increasingly tight tolerances, a flow-like policy must either accumulate sufficient latent-space contraction across its  $K$  refinement steps or allow individual steps to become increasingly ill-conditioned.

**Corollary 16** ( $K$ -step precision tradeoff). *Assume the decoder is a  $K$ -step composition  $F^{(K)} = \Phi_{K-1} \circ \dots \circ \Phi_0$ , where each  $\Phi_t$  is a  $C^1$  diffeomorphism and there exist constants  $\lambda_t > 0$  such that  $\sigma_{\min}(J\Phi_t(z)) \geq \lambda_t$  for all  $z$ . Then the overall map is one-to-one (no folding) and*

$\sigma_*(\delta) \geq \inf_{z \in Z_\delta} \sigma_{\min}(JF^{(K)}(z)) \geq \prod_{t=0}^{K-1} \lambda_t$ . Then, for all  $0 < \delta \leq \bar{\delta}$ ,

$$H_\theta^{(K)}(s; \delta) \geq 1 - C_{\mathcal{M}} \rho_Z^{\max} \left( \prod_{t=0}^{K-1} \lambda_t \right)^{-d} \delta^{d-k}.$$

In particular, if  $\lambda_t \geq \lambda \in (0, 1]$  for all  $t$ , then  $H_\theta^{(K)}(s; \delta) \geq 1 - C_{\mathcal{M}} \rho_Z^{\max} \lambda^{-dK} \delta^{d-k}$ . A necessary condition to bound the hallucination rate  $H_\theta^{(K)}(s; \delta) \leq \eta \in (0, 1)$  is

$$K \geq \frac{1}{d \log(1/\lambda)} \left[ (d-k) \log \frac{1}{\delta} + \log \frac{1-\eta}{C_{\mathcal{M}} \rho_Z^{\max}} \right]. \quad (5)$$

Note: the bound is vacuous when the right-hand side is negative.

**Implications for VLAs.** In this regime of contact-rich tasks, we again see the double-edged nature of smoothness. Intuitively, the policy *should* concentrate probability mass onto the safe action manifold rather than preserve spurious variance that gives rise to action hallucinations. However, there is a cost. Theorem 15 shows that achieving this requires either Jacobian collapse or folding. Both make the latent space a poor coordinate system for optimization (e.g., to find action chunks that achieve an objective). A possible path around the precision barrier is to *project* the VLA’s proposed action back onto the task’s feasible contact manifold (e.g., via constraint solving, low-level controller, or using external sensing like tactile feedback) or *parameterize* the manifold (e.g., an atlas of local charts [18]) so decoded actions stay on-manifold by construction.

Corollary 16 suggests the iterative nature of modern flow and diffusion policies is not solely about sampling from complex action distributions, but rather, about decomposing an effectively singular projection into a product of gentle, well-behaved steps. The dependence on  $\delta$  enters only through a  $\log(1/\delta)$  factor, so the required number of refinement steps grows only logarithmically with tolerance. Interestingly, very recent empirical evidence [36] supports this view and suggest that the advantage of diffusion/flow-style policies is not driven by distribution learning per se. Rather, robust performance on challenging contact-rich tasks is strongly associated with iterative computation and stochasticity injection [36].

## V. HIGH-LEVEL PLAN HALLUCINATIONS

This section builds on the previous analysis of one-step action generation and extends it to long-horizon goal achievement. We develop a theoretical framework that complements empirical findings showing that VLAs/VLMs suffer sharp performance degradation on long-horizon tasks (e.g., [6, 52, 46, 25]) and recent explorations into test-time compute (e.g., [25, 48]).

We begin by fixing a task instance  $I = (\mathcal{E}, s_0, \mathcal{G}, T)$  with deterministic dynamics  $\mathcal{T}$  and defining time-bounded backward-reachable sets,  $\Sigma_0 := \mathcal{G}$ ,  $\Sigma_t := \{s \in \mathcal{S} : \exists a \in \mathcal{A} \text{ s.t. } f_{\text{phys}}(s, a) = 1 \text{ and } \mathcal{T}(s, a) \in \Sigma_{t-1}\}$  for  $t \geq 1$ . Thus,  $s \in \Sigma_t$  means that from state  $s$  there exists a physically-valid action that lands in a state from which the goal

is reachable in  $t$  further steps<sup>1</sup>. For a state  $s$  and remaining horizon  $t \geq 1$  define the *progress set*,  $\mathcal{A}_{\text{prog}}(s, t) := \{a \in \mathcal{A} : f_{\text{phys}}(s, a) = 1 \text{ and } \mathcal{T}(s, a) \in \Sigma_{t-1}\}$ . By construction,  $s \in \Sigma_t$  if and only if  $\mathcal{A}_{\text{prog}}(s, t) \neq \emptyset$ , and  $\mathcal{A}_{\text{prog}}(s, t) \subseteq \mathcal{A}_{\text{safe}}(s)$ , i.e., progress actions are a subset of safe actions.

**Lemma 17** (Horizon Barrier). *Let  $(S_t)_{t=0}^T$  be the rollout from  $s_0$ . Define  $p_t(s) := \Pr_{Z \sim p_Z} [\pi_\theta(s, Z) \in \mathcal{A}_{\text{prog}}(s, t)]$  and  $\gamma_t := \sup_{s \in \Sigma_t} p_t(s)$ . Then the rollout success probability factorizes and is upper bounded by*

$$H_{\pi_\theta}^{\text{plan}}(I) \geq 1 - \prod_{t=1}^T \gamma_t.$$

In particular, if  $\gamma_t \leq \gamma < 1$  for all  $t$ , then  $\Pr[f_{\text{plan}}(s_0, \tau_\theta) = 1] \leq \gamma^T$  and  $H_{\pi_\theta}^{\text{plan}}(I) \geq 1 - \gamma^T$ .

Lemma 17 (proof in Appendix C-A) formalizes the horizon barrier as a *compounding reachability bottleneck*. The idea is intuitive and well-known in robotics [39]: a length- $T$  valid rollout requires sampling a progress action at every step, so success is a product of conditional progress factors. Even if each  $\gamma_t$  is only slightly below one, their product decays rapidly with horizon. This connects directly to the topological and precision barriers since both reduce per-step progress probability and the deficit compounds with  $T$  (also see the discussion in Appendix C-F on action chunking).

Now suppose that a VLA can expend *test-time compute* to verify actions/plans (e.g., RoboMonkey [25], [9]). It can then reduce plan hallucination by checking candidates and abstaining if all fail. Essentially, verification enables the VLA to increase the per-step probability of selecting an action in the progress set. We formalize this setting with a framework for planning with verification.

Fix a finite plan library  $\{\tau^1, \dots, \tau^N\} \subseteq \mathcal{A}^T$  and let  $V := \{i \in \{1, \dots, N\} : f_{\text{plan}}(s_0, \tau^i) = 1\}$  denote the valid index set for instance  $I$ . A *verification-guided planner* runs for at most  $q$  rounds. At round  $j$ , based on past verifier feedback, it chooses a proposal distribution  $Q_j$  over  $\{1, \dots, N\}$ , samples  $J_j \sim Q_j$ , queries a (possibly randomized) verifier  $\tilde{f}_{\text{plan}}(s_0, \tau^{J_j}) \in \{0, 1\}$ , and outputs the first plan accepted by the verifier. If no plan is accepted in  $q$  rounds, it outputs an abstention symbol  $\perp$ .

Assume the verifier has false-positive and false-negative rates bounded by  $\varepsilon_{\text{fp}}, \varepsilon_{\text{fn}} \in [0, 1]$ . Let  $c := 1 - \varepsilon_{\text{fn}}$  denote the minimum true-accept probability on valid plans. Define the planner’s hallucination and abstention probabilities:

$$\begin{aligned} H(I) &:= \Pr[\hat{\tau} \neq \perp \wedge f_{\text{plan}}(s_0, \hat{\tau}) = 0], \\ A(I) &:= \Pr[\hat{\tau} = \perp]. \end{aligned}$$

The planner’s valid-output probability is  $S(I) = 1 - A(I) - H(I)$ . Note that plan hallucination here is slightly different than in Lemma 17 due to the possibility of abstentions. We focus on the design of  $(\alpha, \beta)$ -reliable VLAs, defined below.

<sup>1</sup>If one wishes to interpret  $\Sigma_t$  as “reachable within  $t$  steps” rather than “in exactly  $t$  steps,” it suffices to assume the action set includes a physically-valid *stop/no-op* action that keeps the state unchanged.

**Definition 18**  $((\alpha, \beta)$ -reliability). Fix targets  $\alpha, \beta \in [0, 1]$  with  $\alpha + \beta \leq 1$ . We say the planner is  $(\alpha, \beta)$ -reliable on instance  $I$  if  $H(I) \leq \alpha$  and  $A(I) \leq \beta$ . Equivalently, an  $(\alpha, \beta)$ -reliable planner guarantees a valid plan output with probability at least  $S(I) = 1 - A(I) - H(I) \geq 1 - \alpha - \beta$ .

**Definition 19** (Conditional valid-mass schedule). Let  $C_{j-1}$  denote the event that the planner reaches round  $j$  (i.e., no acceptance occurred in rounds  $1, \dots, j-1$ ). Define the conditional valid-mass at round  $j$  by  $\rho_j := \Pr[J_j \in V \mid C_{j-1}]$ . We refer to  $(\rho_j)_{j=1}^q$  as the planner’s amplification schedule.

**Lemma 20** (Reliability search-budget window). Consider any verification-guided planner with budget  $q$  and verifier error rates  $(\varepsilon_{\text{fp}}, \varepsilon_{\text{fn}})$ , and let  $c := 1 - \varepsilon_{\text{fn}}$ . Let  $(\rho_j)_{j=1}^q$  be its amplification schedule (Definition 19). Then

$$\begin{aligned} H(I) &\leq \varepsilon_{\text{fp}} \sum_{j=1}^q \Pr[C_{j-1}] (1 - \rho_j) \leq q \varepsilon_{\text{fp}} \\ A(I) &\leq \prod_{j=1}^q (1 - c \rho_j). \end{aligned}$$

Consequently, the planner is certified to be  $(\alpha, \beta)$ -reliable whenever  $q \varepsilon_{\text{fp}} \leq \alpha$  and  $\prod_{j=1}^q (1 - c \rho_j) \leq \beta$ .

Lemma 20 (proof in Appendix C-B) separates *verifier-limited* and *planner-limited* effects. Each additional verifier query is *not a free-lunch*: it creates a chance to accept a true valid plan, but it also *increases* the worst-case (upper-bounded) cumulative risk of a hallucination. The product bound shows that abstention decreases only when the planner can make  $\rho_j$  large enough and fast enough, *before* the hallucination-limited budget  $q$  is exhausted. A natural follow-up question is how fast does a planner need to grow  $\rho_j$ ? The following theorem provides an answer for long-horizon tasks.

**Theorem 21** (Amplification-rate to beat the horizon barrier). Consider a verification-guided planner with verifier error rates  $(\varepsilon_{\text{fp}}, \varepsilon_{\text{fn}})$ , amplification schedule  $(\rho_j)_{j=1}^q$  (Definition 19) and targets  $(\alpha, \beta)$ -reliability. Let  $c := 1 - \varepsilon_{\text{fn}}$ . Then, any  $(\alpha, \beta)$ -reliable planner must satisfy  $\sum_{j=1}^q \rho_j \geq 1 - \alpha - \beta$ . Assume the horizon barrier yields an exponentially small initial valid-plan mass  $\rho_1 \leq \gamma^T$  for some  $\gamma \in (0, 1)$ .

**(i) Polynomial amplification is insufficient.** If  $\rho_j \leq \rho_1 j^p$  for some  $p \geq 0$  and all  $j \leq q$ , then

$$\sum_{j=1}^q \rho_j \leq \rho_1 \sum_{j=1}^q j^p \leq \gamma^T \cdot \frac{(q+1)^{p+1} - 1}{p+1}.$$

Consequently, meeting the necessary condition  $\sum_{j=1}^q \rho_j \geq 1 - \alpha - \beta$  requires

$$q \geq \left(1 + \frac{(p+1)(1 - \alpha - \beta)}{\gamma^T}\right)^{\frac{1}{p+1}} - 1,$$

which is exponential in  $T$  for constant  $\gamma \in (0, 1)$ .

**(ii) Geometric amplification is sufficient** (if within the verifier budget). If  $\rho_j \geq \rho_1 r^{j-1}$  for all  $j \leq q$  for some  $r > 1$ , then

$$\sum_{j=1}^q \rho_j \geq \rho_1 \sum_{j=1}^q r^{j-1} = \rho_1 \cdot \frac{r^q - 1}{r - 1}.$$

In particular, a sufficient condition for  $(\alpha, \beta)$ -reliability is

$$q \varepsilon_{\text{fp}} \leq \alpha \quad \text{and} \quad \rho_1 \cdot \frac{r^q - 1}{r - 1} \geq \frac{1}{c} \log\left(\frac{1}{\beta}\right).$$

Hence, geometric amplification requires  $q = \Theta(\log(1/\rho_1))$ . In regimes where  $\rho_1 \approx \gamma^T$  (as suggested by the rollout factorization), this gives  $q = \Theta(T)$ .

Theorem 21 (proof in Appendix C-E) highlights a feasibility constraint. When the horizon barrier makes the initial valid mass small ( $\rho_1 \leq \gamma^T$ ), any amplification that grows only polynomially with the number of rounds (e.g., simple accept/reject) cannot accumulate enough valid mass without *exponentially* many queries. Any certified  $(\alpha, \beta)$ -reliable planner must also satisfy  $q \leq \alpha/\varepsilon_{\text{fp}}$  (Lemma 20). If  $\varepsilon_{\text{fp}}$  is bounded away from zero, then for sufficiently large  $T$  there is *no*  $q$  satisfying both constraints; the feasibility window can *close*. In contrast, geometric (exponential-in- $j$ ) amplification grows valid mass multiplicatively and can reach the abstention threshold quickly enough.

**Implications for VLAs.** Our theoretical analysis above is simple but provides us with key takeaways. First, long-run planning is difficult because success is a product of conditional progress factors. This problem has been long recognized in robotics and remains applicable to contemporary VLAs. A practical (and historically natural) way to address the horizon barrier is to leverage hierarchy, e.g., verify and replan at intermediate semantic or skill boundaries, which turns one length- $T$  rare-event into many shorter-horizon problems.

The verification-guided framework in Lemma 20 clarifies what test-time compute can and cannot buy with noisy verifiers. The algorithmic problem is not merely to “sample more” or “verify more,” but to use the *limited* verification budget to *rapidly increase* the conditional valid mass  $\rho_j$  of the proposals that remain under consideration. The prescriptive message of Theorem 21 is that adaptation must be *multiplicative*. In robotics, gains often come from exploiting structure; rather than treating verification as a binary filter on full trajectories, planners use partial constraints or intermediate progress tests to prune large families of continuations at once (tree search, branch-and-bound, early collision checking). These methodologies have been recently adopted in LLMs (e.g., [47, 54, 42]) and are finding their way back to robotics via VLAs [48, 53]. Our abstraction does not model this structure explicitly, but it highlights why such structure matters; verifier interaction should grow  $\rho_j$  fast enough to beat the horizon barrier.

## VI. CONCLUSIONS, DISCUSSION, AND FUTURE WORK

Taken together, our results suggest that robust VLAs will not emerge from scale alone. The challenge is *structural*: hallucination-free and successful behavior lives on disconnected

and thin subsets of action space, and long horizons turn small local errors into global failures. Our analysis points to design principles more specific than “scale the data” or “add a verifier”. Topology calls for discrete structure to represent disconnected feasible behaviors. Precision favors allocating computation to iterative refinement (or projection) within a chosen mode to reliably hit thin feasible sets, possibly with a properly designed/learned action space. Planning requires pairing verification with adaptive, feedback-driven proposal mechanisms, rather than one-shot accept/reject tests.

The emerging empirical trend in frontier systems [26, 35, 15] is consistent with our findings. For example,  $\pi_{0.5}$  [16] samples discrete subtasks along with a generative action head, which can potentially mitigate the topology barrier. Alpamayo-R1 [35] uses a flow-matching trajectory decoder to produce a control-based representation of *kinematically-feasible* waypoints (the continuous output manifold). Our action hallucination theory provides a lens to sharpen this trend: we should design VLA systems so that test-time computation is spent on multiplicative amplification of valid behavior under controlled verification error, and structure robot model architectures to make that amplification possible.

**Limitations and future work.** We view this work as a step toward a broader theory of VLAs and RFMs. For tractability, we assume deterministic dynamics and abstract away perception, partial observability, memory, and stochasticity—extending our theory view to consider these elements is important. Our verification-guided planning model also simplifies planning and verification; richer models could tighten amplification requirements and yield sharper algorithmic guidance. Beyond verification, future work can examine other reasoning approaches [49, 26, 35]. Finally, it would be interesting to extend our theory towards task distributions and to training-time interventions that systematically reduce hallucinations. We believe progress along these lines can guide the development of next-generation VLAs that are not only more capable, but more *trustworthy*.

#### ACKNOWLEDGMENTS

This research / project is supported by the National Research Foundation, Singapore, under its Thematic Competitive Research Programme 2025 (NRF-T-CRP-2025-0003). The authors would also like to acknowledge support from the Google Foundation.

#### REFERENCES

- [1] Michael Ahn, Anthony Brohan, Noah Brown, Yevgen Chebotar, Omar Cortes, Byron David, Chelsea Finn, Chuyuan Fu, Keerthana Gopalakrishnan, Karol Hausman, Alex Herzog, Daniel Ho, Jasmine Hsu, Julian Ibarz, Brian Ichter, Alex Irpan, Eric Jang, Rosario Jauregui Ruano, Kyle Jeffrey, Sally Jesmonth, Nikhil Joshi, Ryan Julian, Dmitry Kalashnikov, Yuheng Kuang, Kuang-Huei Lee, Sergey Levine, Yao Lu, Linda Luu, Carolina Parada, Peter Pastor, Jornell Quiambao, Kanishka Rao, Jarek Rettinghouse, Diego Reyes, Pierre Sermanet, Nicolas Sievers, Clayton Tan, Alexander Toshev, Vincent Vanhoucke, Fei Xia, Ted Xiao, Peng Xu, Sichun Xu, Mengyuan Yan, and Andy Zeng. Do as i can and not as i say: Grounding language in robotic affordances. In *arXiv preprint arXiv:2204.01691*, 2022.
- [2] Kevin Black, Noah Brown, Danny Driess, Adnan Esmail, Michael Equi, Chelsea Finn, Niccolò Fusai, Lachy Groom, Karol Hausman, Brian Ichter, et al.  $\pi_0$ : A vision-language-action flow model for general robot control. *arXiv preprint arXiv:2410.24164*, 2024.
- [3] Piermarco Cannarsa, Marc-Olivier Czarnecki, et al. Minkowski content for reachable sets. *manuscripta mathematica*, 131(3):507–530, 2010.
- [4] John Canny. *Complexity of Robot Motion Planning*. PhD thesis, MIT, 1988.
- [5] Cheng Chi, Siyuan Feng, Yilun Du, Zhenjia Xu, Eric Cousineau, Benjamin Burchfiel, and Shuran Song. Diffusion policy: Visuomotor policy learning via action diffusion. In *Proceedings of Robotics: Science and Systems (RSS)*, 2023.
- [6] Liu Dai, Haina Wang, Weikang Wan, and Hao Su. Mani-taskgen: A comprehensive task generator for benchmarking and improving vision-language agents on embodied decision-making. 2025.
- [7] Xiaobing Dai, Zewen Yang, Dian Yu, Fangzhou Liu, Hamid Sadeghian, Sami Haddadin, and Sandra Hirche. Safeflow: Safe robot motion planning with flow matching via control barrier functions, 2025.
- [8] Zeyu Feng, Hao Luan, Kevin Yuchen Ma, and Harold Soh. Diffusion meets options: Hierarchical generative skill composition for temporally-extended tasks. In *2025 IEEE International Conference on Robotics and Automation (ICRA)*, pages 10854–10860, 2025.
- [9] Huy Ha, Pete Florence, and Shuran Song. Scaling up and distilling down: Language-guided robot skill acquisition. In *Conference on Robot Learning*, pages 3766–3777. PMLR, 2023.
- [10] Ce Hao, Xuanran Zhai, Yaohua Liu, and Harold Soh. Abstracting robot manipulation skills via mixture-of-experts diffusion policies. In *The Fourteenth International Conference on Learning Representations*, 2026.
- [11] Kris Hauser and Jean-Claude Latombe. Multi-modal motion planning in non-expansive spaces. *The International Journal of Robotics Research*, 29(7):897–915, 2010.
- [12] D. Hsu, J.-C. Latombe, and R. Motwani. Path planning in expansive configuration spaces. In *Proceedings of International Conference on Robotics and Automation*, volume 3, pages 2719–2726, 1997.
- [13] David Hsu, Jean-Claude Latombe, and Hanna Kurniawati. On the probabilistic foundations of probabilistic roadmap planning. *The International Journal of Robotics Research*, 25(7):627–643, 2006.
- [14] Lei Huang, Weijiang Yu, Weitao Ma, Weihong Zhong, Zhangyin Feng, Haotian Wang, Qianglong Chen, Weihua Peng, Xiaocheng Feng, Bing Qin, and Ting Liu. A survey on hallucination in large language models: Principles,

taxonomy, challenges, and open questions. *ACM Trans. Inf. Syst.*, 43(2), January 2025. ISSN 1046-8188.

[15] Physical Intelligence, Ali Amin, Raichelle Aniceto, Ashwin Balakrishna, Kevin Black, Ken Conley, Grace Conners, James Darpinian, Karan Dhabalia, Jared DiCarlo, Danny Driess, Michael Equi, Adnan Esmail, Yunhao Fang, Chelsea Finn, Catherine Glossop, Thomas Godden, Ivan Goryachev, Lachy Groom, Hunter Hancock, Karol Hausman, Gashon Hussein, Brian Ichter, Szymon Jakubczak, Rowan Jen, Tim Jones, Ben Katz, Liyiming Ke, Chandra Kuchi, Marinda Lamb, Devin LeBlanc, Sergey Levine, Adrian Li-Bell, Yao Lu, Vishnu Mano, Mohith Mothukuri, Suraj Nair, Karl Pertsch, Allen Z. Ren, Charvi Sharma, Lucy Xiaoyang Shi, Laura Smith, Jost Tobias Springenberg, Kyle Stachowicz, Will Stoeckle, Alex Swerdfloor, James Tanner, Marcel Torne, Quan Vuong, Anna Walling, Haohuan Wang, Blake Williams, Sukwon Yoo, Lili Yu, Ury Zhilinsky, and Zhiyuan Zhou.  $\pi_{0.6}^*$ : a vla that learns from experience, 2025.

[16] Physical Intelligence, Kevin Black, Noah Brown, James Darpinian, Karan Dhabalia, Danny Driess, Adnan Esmail, Michael Equi, Chelsea Finn, Niccolo Fusai, et al.  $\pi_{0.5}$ : a vision-language-action model with open-world generalization. *arXiv preprint arXiv:2504.16054*, 2025.

[17] Thibaut Issenhuth, Ugo Tanielian, Jeremie Mary, and David Picard. Unveiling the latent space geometry of push-forward generative models. In Andreas Krause, Emma Brunskill, Kyunghyun Cho, Barbara Engelhardt, Sivan Sabato, and Jonathan Scarlett, editors, *Proceedings of the 40th International Conference on Machine Learning*, volume 202 of *Proceedings of Machine Learning Research*, pages 14422–14444. PMLR, 23–29 Jul 2023.

[18] Léonard Jaillet and Josep M Porta. Path planning under kinematic constraints by rapidly exploring manifolds. *IEEE Transactions on Robotics*, 29(1):105–117, 2012.

[19] Ziwei Ji, Nayeon Lee, Rita Frieske, Tiezheng Yu, Dan Su, Yan Xu, Etsuko Ishii, Ye Jin Bang, Andrea Madotto, and Pascale Fung. Survey of hallucination in natural language generation. *ACM Comput. Surv.*, 55(12), March 2023. ISSN 0360-0300.

[20] Xiaogang Jia, Denis Blessing, Xinkai Jiang, Moritz Reuss, Atalay Donat, Rudolf Lioutikov, and Gerhard Neumann. Towards diverse behaviors: A benchmark for imitation learning with human demonstrations. In *The Twelfth International Conference on Learning Representations*, 2024.

[21] Herman Kahn and Theodore E Harris. Estimation of particle transmission by random sampling. *National Bureau of Standards applied mathematics series*, 12:27–30, 1951.

[22] Adam Tauman Kalai and Santosh S. Vempala. Calibrated language models must hallucinate. In *Proceedings of the 56th Annual ACM Symposium on Theory of Computing (STOC)*, 2024.

[23] Mahyar Khayatkhoei, Maneesh K. Singh, and Ahmed Elgammal. Disconnected manifold learning for generative adversarial networks. In Samy Bengio, Hanna Wallach, Hugo Larochelle, Kristen Grauman, Nicolò Cesa-Bianchi, and Roman Garnett, editors, *Advances in Neural Information Processing Systems 31*, pages 7354–7364. Curran Associates, Inc., 2018.

[24] Moo Jin Kim, Karl Pertsch, Siddharth Karamchetti, Ted Xiao, Ashwin Balakrishna, Suraj Nair, Rafael Rafailov, Ethan Foster, Grace Lam, Pannag Sanketi, Quan Vuong, Thomas Kollar, Benjamin Burchfiel, Russ Tedrake, Dorsa Sadigh, Sergey Levine, Percy Liang, and Chelsea Finn. Openvla: An open-source vision-language-action model, 2024.

[25] Jacky Kwok, Christopher Agia, Rohan Sinha, Matt Foutter, Shulu Li, Ion Stoica, Azalia Mirhoseini, and Marco Pavone. Robomonkey: Scaling test-time sampling and verification for vision-language-action models. In *Second Workshop on Out-of-Distribution Generalization in Robotics at RSS 2025*, 2025.

[26] Jason Lee, Jiafei Duan, Haoquan Fang, Yuquan Deng, Shuo Liu, Boyang Li, Bohan Fang, Jieyu Zhang, Yi Ru Wang, Sangho Lee, Winson Han, Wilbert Pumacay, Angelica Wu, Rose Hendrix, Karen Farley, Eli VanderBilt, Ali Farhadi, Dieter Fox, and Ranjay Krishna. Molmoact: Action reasoning models that can reason in space, 2025.

[27] Sheng Liu, Haotian Ye, and James Zou. Reducing hallucinations in large vision-language models via latent space steering. In *The Thirteenth International Conference on Learning Representations*, 2025.

[28] Songming Liu, Lingxuan Wu, Bangguo Li, Hengkai Tan, Huayu Chen, Zhengyi Wang, Ke Xu, Hang Su, and Jun Zhu. RDT-1b: a diffusion foundation model for bimanual manipulation. In *The Thirteenth International Conference on Learning Representations*, 2025.

[29] Tomas Lozano-Perez, Matthew T Mason, and Russell H Taylor. Automatic synthesis of fine-motion strategies for robots. *The International Journal of Robotics Research*, 3(1):3–24, 1984.

[30] Tomas Lozano-Pérez. Spatial planning: A configuration space approach. *IEEE Transactions on Computers*, C-32(2):108–120, 1979.

[31] Matthew Mason. The mechanics of manipulation. In *Proceedings. 1985 IEEE International Conference on Robotics and Automation*, volume 2, pages 544–548. IEEE, 1985.

[32] Matthew T Mason. Compliance and force control for computer controlled manipulators. *IEEE Transactions on Systems, Man, and Cybernetics*, 11(6):418–432, 1981.

[33] Pertti Mattila. Rectifiability; a survey. *arXiv preprint arXiv:2112.00540*, 2021.

[34] NVIDIA, :, Johan Bjorck, Fernando Castañeda, Nikita Cherniadev, Xingye Da, Runyu Ding, Linxi "Jim" Fan, Yu Fang, Dieter Fox, Fengyuan Hu, Spencer Huang, Joel Jang, Zhenyu Jiang, Jan Kautz, Kaushil Kundalia, Lawrence Lao, Zhiqi Li, Zongyu Lin, Kevin Lin, Guilin Liu, Edith Llontop, Loic Magne, Ajay Mandlekar, Avnish Narayan, Soroush Nasiriany, Scott Reed, You Liang Tan,

Guanzhi Wang, Zu Wang, Jing Wang, Qi Wang, Jiannan Xiang, Yuqi Xie, Yinzen Xu, Zhenjia Xu, Seonghyeon Ye, Zhiding Yu, Ao Zhang, Hao Zhang, Yizhou Zhao, Ruijie Zheng, and Yuke Zhu. Gr00t n1: An open foundation model for generalist humanoid robots, 2025.

[35] NVIDIA, : Yan Wang, Wenjie Luo, Junjie Bai, Yulong Cao, Tong Che, Ke Chen, Yuxiao Chen, Jenna Diamond, Yifan Ding, Wenhao Ding, Liang Feng, Greg Heinrich, Jack Huang, Peter Karkus, Boyi Li, Pinyi Li, Tsung-Yi Lin, Dongran Liu, Ming-Yu Liu, Langechuan Liu, Zhijian Liu, Jason Lu, Yunxiang Mao, Pavlo Molchanov, Lindsey Pavao, Zhenghao Peng, Mike Ranzinger, Ed Schmerling, Shida Shen, Yunfei Shi, Sarah Tariq, Ran Tian, Tilman Wekel, Xinshuo Weng, Tianjun Xiao, Eric Yang, Xiaodong Yang, Yurong You, Xiaohui Zeng, Wenyuan Zhang, Boris Ivanovic, and Marco Pavone. Alpamayo-r1: Bridging reasoning and action prediction for generalizable autonomous driving in the long tail, 2026.

[36] Chaoyi Pan, Giri Anantharaman, Nai-Chieh Huang, Claire Jin, Daniel Pfrommer, Chenyang Yuan, Frank Permenter, Guannan Qu, Nicholas Boffi, Guanya Shi, and Max Simchowitz. Much ado about noising: Dispelling the myths of generative robotic control, 2025.

[37] George Papamakarios, Eric Nalisnick, Danilo Jimenez Rezende, Shakir Mohamed, and Balaji Lakshminarayanan. Normalizing flows for probabilistic modeling and inference. *Journal of Machine Learning Research*, 22(57):1–64, 2021.

[38] John H Reif. Complexity of the mover’s problem and generalizations. In *20th Annual Symposium on Foundations of Computer Science (sfcs 1979)*, pages 421–427. IEEE Computer Society, 1979.

[39] Stéphane Ross and Drew Bagnell. Efficient reductions for imitation learning. In *Proceedings of the thirteenth international conference on artificial intelligence and statistics*, pages 661–668. JMLR Workshop and Conference Proceedings, 2010.

[40] Reuven Y Rubinstein and Dirk P Kroese. *The cross-entropy method: a unified approach to combinatorial optimization, Monte-Carlo simulation and machine learning*. Springer Science & Business Media, 2004.

[41] Antoine Salmona, Valentin De Bortoli, Julie Delon, and Agnes Desolneux. Can push-forward generative models fit multimodal distributions? *Advances in Neural Information Processing Systems*, 35:10766–10779, 2022.

[42] Charlie Snell, Jaehoon Lee, Kelvin Xu, and Aviral Kumar. Scaling llm test-time compute optimally can be more effective than scaling model parameters, 2024.

[43] Vincent Stimper, Bernhard Schölkopf, and Jose Miguel Hernández-Lobato. Resampling base distributions of normalizing flows. In Gustau Camps-Valls, Francisco J. R. Ruiz, and Isabel Valera, editors, *Proceedings of The 25th International Conference on Artificial Intelligence and Statistics*, volume 151 of *Proceedings of Machine Learning Research*, pages 4915–4936. PMLR, 28–30 Mar 2022.

[44] Ugo Tanielian, Thibaut Issenhuth, Elvis Dohmatob, and Jeremie Mary. Learning disconnected manifolds: a no GAN’s land. In Hal Daumé III and Aarti Singh, editors, *Proceedings of the 37th International Conference on Machine Learning*, volume 119 of *Proceedings of Machine Learning Research*, pages 9418–9427. PMLR, 13–18 Jul 2020.

[45] Ziwei Xu, Sanjay Jain, and Mohan Kankanhalli. Hallucination is inevitable: An innate limitation of large language models, 2025.

[46] Rui Yang, Hanyang Chen, Junyu Zhang, Mark Zhao, Cheng Qian, Kangrui Wang, Qineng Wang, Teja Venkat Koripella, Marziyeh Movahedi, Manling Li, Heng Ji, Huan Zhang, and Tong Zhang. Embodiedbench: Comprehensive benchmarking multi-modal large language models for vision-driven embodied agents. In *Forty-second International Conference on Machine Learning*, 2025.

[47] Shunyu Yao, Dian Yu, Jeffrey Zhao, Izhak Shafran, Thomas L. Griffiths, Yuan Cao, and Karthik Narasimhan. Tree of thoughts: deliberate problem solving with large language models. In *Proceedings of the 37th International Conference on Neural Information Processing Systems*, NIPS ’23, Red Hook, NY, USA, 2023. Curran Associates Inc.

[48] Jaesik Yoon, Hyeonseo Cho, Doojin Baek, Yoshua Bengio, and Sungjin Ahn. Monte carlo tree diffusion for system 2 planning. In *Forty-second International Conference on Machine Learning*, 2025.

[49] Michał Zawalski, William Chen, Karl Pertsch, Oier Mees, Chelsea Finn, and Sergey Levine. Robotic control via embodied chain-of-thought reasoning. In *8th Annual Conference on Robot Learning*, 2024.

[50] Xuanran Zhai, Qianyou Zhao, Qiaojun Yu, and Ce Hao. Vfp: Variational flow-matching policy for multi-modal robot manipulation, 2025.

[51] Qinglun Zhang, Zhen Liu, Haoqiang Fan, Guanghui Liu, Bing Zeng, and Shuaicheng Liu. Flowpolicy: Enabling fast and robust 3d flow-based policy via consistency flow matching for robot manipulation. 2024.

[52] Shiduo Zhang, Zhe Xu, Peiju Liu, Xiaopeng Yu, Yuan Li, Qinghui Gao, Zhaoye Fei, Zhangyue Yin, Zuxuan Wu, Yu-Gang Jiang, and Xipeng Qiu. Vlabench: A large-scale benchmark for language-conditioned robotics manipulation with long-horizon reasoning tasks. In *Proceedings of the IEEE/CVF International Conference on Computer Vision (ICCV)*, pages 11142–11152, October 2025.

[53] Zirui Zhao, Wee Sun Lee, and David Hsu. Large language models as commonsense knowledge for large-scale task planning. In *Proceedings of the 37th International Conference on Neural Information Processing Systems*, NIPS ’23, Red Hook, NY, USA, 2023. Curran Associates Inc.

[54] Andy Zhou, Kai Yan, Michal Shlapentokh-Rothman, Haohan Wang, and Yu-Xiong Wang. Language agent tree

search unifies reasoning acting and planning in language models, 2023.

[55] Brianna Zitkovich, Tianhe Yu, Sichun Xu, Peng Xu, Ted Xiao, Fei Xia, Jialin Wu, Paul Wohlhart, Stefan Welker, Ayzaan Wahid, Quan Vuong, Vincent Vanhoucke, Huong Tran, Radu Soricut, Anikait Singh, Jaspiar Singh, Pierre Sermanet, Pannag R. Sanketi, Grecia Salazar, Michael S. Ryoo, Krista Reymann, Kanishka Rao, Karl Pertsch, Igor Mordatch, Henryk Michalewski, Yao Lu, Sergey Levine, Lisa Lee, Tsang-Wei Edward Lee, Isabel Leal, Yuheng Kuang, Dmitry Kalashnikov, Ryan Julian, Nikhil J. Joshi, Alex Irpan, Brian Ichter, Jasmine Hsu, Alexander Herzog,

Karol Hausman, Keerthana Gopalakrishnan, Chuyuan Fu, Pete Florence, Chelsea Finn, Kumar Avinava Dubey, Danny Driess, Tianli Ding, Krzysztof Marcin Choromanski, Xi Chen, Yevgen Chebotar, Justice Carbalal, Noah Brown, Anthony Brohan, Montserrat Gonzalez Arenas, and Kehang Han. Rt-2: Vision-language-action models transfer web knowledge to robotic control. In Jie Tan, Marc Toussaint, and Kourosh Darvish, editors, *Proceedings of The 7th Conference on Robot Learning*, volume 229 of *Proceedings of Machine Learning Research*, pages 2165–2183. PMLR, 06–09 Nov 2023.

# SUPPLEMENTARY MATERIAL FOR “ACTION HALLUCINATION IN GENERATIVE VISUAL-LANGUAGE-ACTION MODELS”

## APPENDIX A TOPOLOGICAL BARRIER: PROOFS AND ADDITIONAL DETAILS

### A. Proof of Topological Barrier (Lemma 10)

**Lemma 10** (Topological Barrier). *Suppose Assumption 9 holds and there exist  $z_L, z_R \in \mathcal{Z}$  such that  $\pi_\theta(s, z_L) \in U_L$  and  $\pi_\theta(s, z_R) \in U_R$ . Define the seam set,  $\mathcal{Z}_{\text{seam}}(s) := \{z \in \mathcal{Z} : \pi_\theta(s, z) \in \mathcal{A}_{\text{forb}}(s)\}$ . Then  $\mathcal{Z}_{\text{seam}}(s)$  is nonempty and open in  $\mathcal{Z}$ . The hallucination probability at  $s$  is strictly positive:*

$$H_\theta(s) = \Pr_{z \sim p_Z} [z \in \mathcal{Z}_{\text{seam}}(s)] > 0.$$

In other words, no continuous latent-to-action map that covers both safe modes can be hallucination-free at  $s$ .

*Proof:* We fix a state  $s$  and suppress the dependence on  $s$  to avoid clutter.

a) *Nonemptiness.*: By Assumption 3,  $\mathcal{Z}$  is path-connected, so there exists a continuous path  $\gamma : [0, 1] \rightarrow \mathcal{Z}$  with  $\gamma(0) = z_L$  and  $\gamma(1) = z_R$ . Define the action-space path  $g : [0, 1] \rightarrow \mathcal{A}$  by  $g(t) := \pi_\theta(s, \gamma(t))$ . By continuity of  $z \mapsto \pi_\theta(s, z)$ , the map  $g$  is continuous.

By assumption,  $g(0) \in U_L \subseteq \mathcal{A}_{\text{safe}}(s)$  and  $g(1) \in U_R \subseteq \mathcal{A}_{\text{safe}}(s)$ . If  $g(t) \in \mathcal{A}_{\text{safe}}(s)$  for all  $t \in [0, 1]$ , then  $g$  would be a continuous path in  $\mathcal{A}_{\text{safe}}(s)$  connecting a point in  $U_L$  to a point in  $U_R$ , contradicting that  $U_L$  and  $U_R$  are distinct path-connected components of  $\mathcal{A}_{\text{safe}}(s)$  (Assumption 9(i)). Therefore, there exists  $t^* \in (0, 1)$  such that  $g(t^*) \notin \mathcal{A}_{\text{safe}}(s)$ , i.e.,  $g(t^*) \in \mathcal{A}_{\text{forb}}(s)$ . Let  $z^* := \gamma(t^*)$ ; then  $z^* \in \mathcal{Z}_{\text{seam}}(s)$ , so  $\mathcal{Z}_{\text{seam}}(s)$  is nonempty.

b) *Openness.*: By Assumption 9(ii),  $\mathcal{A}_{\text{forb}}(s)$  is open in  $\mathcal{A}$ , and by construction  $\mathcal{Z}_{\text{seam}}(s) = \pi_\theta(s, \cdot)^{-1}(\mathcal{A}_{\text{forb}}(s))$ . Since preimages of open sets under continuous maps are open,  $\mathcal{Z}_{\text{seam}}(s)$  is open in  $\mathcal{Z}$ .

c) *Positive probability.*: Pick  $z^* \in \mathcal{Z}_{\text{seam}}(s)$ . Since  $\mathcal{Z}_{\text{seam}}(s)$  is open in  $\mathcal{Z}$  and  $\mathcal{Z}$  is open in  $\mathbb{R}^d$ , there exists  $r > 0$  such that the closed ball  $K := \overline{B(z^*, r)} \subset \mathcal{Z}_{\text{seam}}(s)$  and  $K \subset \mathcal{Z}$ . By Assumption 3, there exists  $\rho_{\min}(K) > 0$  such that  $\rho_Z(z) \geq \rho_{\min}(K)$  for almost every  $z \in K$ . Hence

$$H_\theta(s) = \Pr[Z \in \mathcal{Z}_{\text{seam}}(s)] \geq \Pr[Z \in K] = \int_K \rho_Z(z) dz \geq \rho_{\min}(K) \text{Vol}(K) > 0.$$

■

### B. Proof of Isoperimetric Lower-Bound (Theorem 12)

Our quantitative bound follows the same isoperimetric / latent pre-image boundary methodology used to prove precision limitations for Lipschitz pushforward generative models [41, 44, 17], but we adapt this methodology to state-conditional action generation and interpret boundary mass as unsafe-action probability under a physically meaningful forbidden buffer assumption, with a local-Lipschitz typical-set correction.

**Theorem 12** (Isoperimetric lower bound on action hallucination). *Fix a state  $s$  satisfying Assumption 11. Let  $Z \sim \mathcal{N}(0, I_d)$  and fix a radius  $R > 0$ . Assume that the latent-to-action head  $z \mapsto \pi_\theta(s, z)$  is  $L$ -Lipschitz on the typical-latent ball  $B_R := \{z \in \mathbb{R}^d : \|z\| \leq R\}$ , i.e.,  $\|\pi_\theta(s, z) - \pi_\theta(s, z')\| \leq L \|z - z'\| \forall z, z' \in B_R$ . Let  $\epsilon := W/L$ .*

*For each safe mode  $U_i$ , define the latent preimage  $V_i := \pi_\theta(s, \cdot)^{-1}(U_i)$  and the in-ball mass  $p_i^{(R)} := \Pr[Z \in V_i \cap B_R]$ . Let  $q(R) = \Pr[\|Z\| > R]$ . Then the hallucination probability at  $s$  satisfies*

$$H_\theta(s) \geq \sum_{i=1}^M \left[ \Phi \left( \Phi^{-1}(p_i^{(R)}) + \epsilon \right) - p_i^{(R)} \right] - q(R), \quad (1)$$

where  $\Phi$  is the CDF of the standard normal distribution.

*Proof:* Fix  $s$  and write  $B_R := \{z \in \mathbb{R}^d : \|z\| \leq R\}$ . Let  $Z \sim \mathcal{N}(0, I_d)$  and let  $\gamma_d(\cdot)$  denote standard Gaussian measure on  $\mathbb{R}^d$ , so that  $\Pr[Z \in E] = \gamma_d(E)$  for measurable  $E$ . Let  $\epsilon := W/L$ .

For each mode  $U_i$ , define  $V_i := \pi_\theta(s, \cdot)^{-1}(U_i)$  and set

$$A_i := V_i \cap B_R, \quad p_i^{(R)} := \gamma_d(A_i).$$

a) *Step 1: Separation of in-ball preimages.*: Fix  $i \neq j$  and take any  $z \in A_i$  and  $z' \in A_j$ . Then  $z, z' \in B_R$ , so Lipschitzness applies:

$$\|\pi_\theta(s, z) - \pi_\theta(s, z')\| \leq L\|z - z'\|.$$

Moreover,  $\pi_\theta(s, z) \in U_i$  and  $\pi_\theta(s, z') \in U_j$ , and Assumption 11(ii) gives  $\text{dist}(U_i, U_j) \geq 2W$ , hence

$$2W \leq \|\pi_\theta(s, z) - \pi_\theta(s, z')\| \leq L\|z - z'\|.$$

Therefore  $\|z - z'\| \geq 2W/L = 2\epsilon$ . Taking the infimum over  $z \in A_i$  and  $z' \in A_j$  yields

$$\text{dist}(A_i, A_j) \geq 2\epsilon.$$

b) *Step 2: Disjoint halos and inclusion in the seam inside  $B_R$ .*: Define the open  $\epsilon$ -halo around  $A_i$  by

$$S_i := \{z \in \mathbb{R}^d : 0 < \text{dist}(z, A_i) < \epsilon\}.$$

*Disjointness.* If  $z \in S_i \cap S_j$ , then there exist  $v_i \in A_i$  and  $v_j \in A_j$  with  $\|z - v_i\| < \epsilon$  and  $\|z - v_j\| < \epsilon$ , so  $\|v_i - v_j\| < 2\epsilon$ , contradicting  $\text{dist}(A_i, A_j) \geq 2\epsilon$ . Thus  $\{S_i\}_{i=1}^M$  are pairwise disjoint.

*Halo points inside  $B_R$  map to forbidden actions.* Take any  $z \in S_i \cap B_R$ . By definition, there exists  $v \in A_i$  with  $\|z - v\| < \epsilon$ . Since  $z, v \in B_R$ , Lipschitzness gives

$$\|\pi_\theta(s, z) - \pi_\theta(s, v)\| \leq L\|z - v\| < L\epsilon = W,$$

and since  $\pi_\theta(s, v) \in U_i$ , we have  $\text{dist}(\pi_\theta(s, z), U_i) < W$ . Also,  $z \notin A_i = V_i \cap B_R$  and  $z \in B_R$  implies  $z \notin V_i$ , hence  $\pi_\theta(s, z) \notin U_i$ . Therefore  $\pi_\theta(s, z) \in \mathcal{A}_{\text{forb}}(s)$  by Assumption 11(ii), and thus  $z \in \mathcal{Z}_{\text{seam}}(s)$ . We conclude

$$\bigcup_{i=1}^M (S_i \cap B_R) \subseteq \mathcal{Z}_{\text{seam}}(s).$$

c) *Step 3: Gaussian isoperimetry.*: Let  $A_i^\epsilon := \{z : \text{dist}(z, A_i) \leq \epsilon\}$  denote the closed  $\epsilon$ -neighborhood. Up to a Gaussian-null boundary,  $S_i = A_i^\epsilon \setminus A_i$ , hence

$$\Pr[Z \in S_i] = \gamma_d(A_i^\epsilon) - \gamma_d(A_i) = \gamma_d(A_i^\epsilon) - p_i^{(R)}.$$

By the Gaussian isoperimetric inequality,

$$\gamma_d(A_i^\epsilon) \geq \Phi(\Phi^{-1}(p_i^{(R)}) + \epsilon),$$

so

$$\Pr[Z \in S_i] \geq \Phi(\Phi^{-1}(p_i^{(R)}) + \epsilon) - p_i^{(R)}.$$

d) *Step 4: Sum halos and apply the tail correction.*: Since the halos  $S_i$  are disjoint,

$$\Pr\left[Z \in \bigcup_{i=1}^M S_i\right] = \sum_{i=1}^M \Pr[Z \in S_i].$$

Moreover,

$$\begin{aligned} \Pr\left[Z \in \bigcup_{i=1}^M (S_i \cap B_R)\right] &= \Pr\left[Z \in \bigcup_{i=1}^M S_i\right] - \Pr\left[Z \in \bigcup_{i=1}^M S_i \cap B_R^c\right] \\ &\geq \Pr\left[Z \in \bigcup_{i=1}^M S_i\right] - \Pr[Z \in B_R^c]. \end{aligned}$$

Combining with Step 2 yields

$$\begin{aligned} H_\theta(s) = \Pr[Z \in \mathcal{Z}_{\text{seam}}(s)] &\geq \Pr\left[Z \in \bigcup_{i=1}^M (S_i \cap B_R)\right] \\ &\geq \sum_{i=1}^M \Pr[Z \in S_i] - \Pr[\|Z\| > R], \end{aligned}$$

and Step 3 gives (1). ■

**Remark: Small  $\epsilon$  regime.** In the situation where  $\epsilon$  is small, we can obtain that

$$H_\theta(s) \geq \epsilon \sum_{i=1}^M \phi(\Phi^{-1}(p_i^{(R)})) - q(R) - O(\epsilon^2), \quad (6)$$

where  $\phi$  is the standard normal PDF. To see this, fix  $i$  and write  $x_i := \Phi^{-1}(p_i^{(R)})$ , so that  $\Phi(x_i) = p_i^{(R)}$ . Taylor's theorem with Lagrange remainder gives

$$\Phi(x_i + \epsilon) = \Phi(x_i) + \epsilon \phi(x_i) + \frac{\epsilon^2}{2} \Phi''(\xi_i)$$

for some  $\xi_i$  between  $x_i$  and  $x_i + \epsilon$ . Since  $\Phi'(x) = \phi(x)$  and  $\Phi''(x) = -x\phi(x)$ , and  $\sup_{x \in \mathbb{R}} |x\phi(x)| = 1/\sqrt{2\pi e}$ , we obtain the uniform bound

$$\Phi(x_i + \epsilon) - p_i^{(R)} = \epsilon \phi(x_i) + O(\epsilon^2) \quad \text{with } |O(\epsilon^2)| \leq \frac{\epsilon^2}{2\sqrt{2\pi e}}.$$

Summing over  $i$  and subtracting  $\Pr[\|Z\| > R]$  yields (6).

**Remark: Optimizing over the typical-set radius  $R$ .** We can tighten the bound in Theorem 12; for any  $R > 0$  such that  $\pi(s, \cdot)$  is Lipschitz on  $B_R$  with constant  $L_R$ , define  $\epsilon_R = W/L_R$ . Then (1) holds with  $\epsilon$  is replaced by  $\epsilon_R$  and  $H_\theta(s)$  is lower bounded by the supremum of the RHS over  $R$ ,

$$H_\theta(s) \geq \sup_{R > 0: L_R < \infty} \left\{ \sum_{i=1}^M \left[ \Phi(\Phi^{-1}(p_i^{(R)}) + \epsilon_R) - p_i^{(R)} \right] - q(R) \right\}$$

## APPENDIX B PRECISION BARRIER: PROOFS AND ADDITIONAL DETAILS

### A. Proof of Precision Barrier (Lemma 14)

We will make use of the following lemma about the volume of tubular neighborhoods, which is based on Theorem A in [3].

**Lemma 22** (Volume of Tubes Around Submanifolds). *Let  $\mathcal{M} \subset \mathbb{R}^d$  be a compact  $C^1$  submanifold of dimension  $k < d$ . Then there exist constants  $C_{\mathcal{M}} > 0$  and  $\bar{\delta} > 0$  such that for all  $0 < \delta \leq \bar{\delta}$ ,*

$$\text{Vol}(\mathcal{M}_\delta) \leq C_{\mathcal{M}} \delta^{d-k},$$

where  $\text{Vol}$  denotes the  $d$ -dimensional Lebesgue measure.

*Proof:* For  $\delta > 0$ ,  $\mathcal{M}_\delta$  is the closed  $\delta$ -neighborhood of  $\mathcal{M}$ :

$$\mathcal{M}_\delta = \overline{B}(\mathcal{M}, \delta) := \{x \in \mathbb{R}^d : \text{dist}(x, \mathcal{M}) \leq \delta\}.$$

Let

$$\omega_m := \text{Vol}_m(B_{\mathbb{R}^m}(0, 1))$$

denote the  $m$ -dimensional Lebesgue volume of the unit Euclidean ball. Since  $\mathcal{M}$  is a compact  $C^1$   $k$ -dimensional submanifold of  $\mathbb{R}^d$ , it is  $k$ -rectifiable [33]. Hence Theorem A [3] applies with  $n = d$  and  $p = k$ , and yields the existence of the (finite) limit

$$\lim_{\delta \rightarrow 0^+} \frac{\text{Vol}(\mathcal{M}_\delta)}{\omega_{d-k} \delta^{d-k}} =: \text{Area}_k(\mathcal{M}),$$

where  $\text{Area}_k(\mathcal{M})$  denotes the intrinsic  $k$ -dimensional surface area of  $\mathcal{M}$  (i.e., the  $k$ -dimensional Hausdorff measure). Define

$$f(\delta) := \frac{\text{Vol}(\mathcal{M}_\delta)}{\omega_{d-k} \delta^{d-k}}.$$

Then  $\lim_{\delta \rightarrow 0^+} f(\delta) = L_{\mathcal{M}}$ . Taking  $\varepsilon = 1$  in the definition of convergence, there exists  $\delta_0 > 0$  such that for all  $0 < \delta < \delta_0$ ,

$$|f(\delta) - L_{\mathcal{M}}| < 1 \quad \Rightarrow \quad f(\delta) < L_{\mathcal{M}} + 1.$$

Set  $\bar{\delta} := \delta_0/2$ . Then for all  $0 < \delta \leq \bar{\delta}$ ,  $f(\delta) \leq L_{\mathcal{M}} + 1$ . Multiplying through gives

$$\text{Vol}(\mathcal{M}_\delta) \leq \underbrace{\omega_{d-k} (L_{\mathcal{M}} + 1)}_{C_{\mathcal{M}}} \delta^{d-k}$$

■

Using Lemma 22, we prove our precision barrier below.

**Lemma 14** (Precision Barrier). *Fix a state  $s$  and adopt Definition 13. Then, there exist constants  $C_{\mathcal{M}} > 0$  and  $\bar{\delta} > 0$  (depending only on  $\mathcal{M}$ ) such that for all  $0 < \delta \leq \bar{\delta}$ ,  $S_{\theta}(s; \delta) \leq C_{\mathcal{M}} \delta^{d-k} \cdot \text{ess sup}_{a \in \mathcal{M}_{\delta}} p(a | s)$ , and hence*

$$H_{\theta}(s; \delta) \geq 1 - C_{\mathcal{M}} \delta^{d-k} \cdot \text{ess sup}_{a \in \mathcal{M}_{\delta}} p(a | s). \quad (2)$$

If  $H_{\theta}(s; \delta) \leq \eta$  for some  $\eta \in (0, 1)$ , then  $\text{ess sup}_{a \in \mathcal{M}_{\delta}} p(a | s) \geq \frac{1-\eta}{C_{\mathcal{M}}} \delta^{-(d-k)}$ .

*Proof:* Fix  $0 < \delta \leq \bar{\delta}$  (where  $\bar{\delta}$  will be chosen below). Since  $\mathcal{A}_{\text{safe}}(s; \delta) \subseteq \mathcal{M}_{\delta}$  and  $p(\cdot | s) \geq 0$ ,

$$S_{\theta}(s; \delta) = \int_{\mathcal{A}_{\text{safe}}(s; \delta)} p(a | s) da \leq \int_{\mathcal{M}_{\delta}} p(a | s) da.$$

Since  $p(a | s) \leq \text{ess sup}_{u \in \mathcal{M}_{\delta}} p(u | s)$  for almost every  $a \in \mathcal{M}_{\delta}$ ,

$$\int_{\mathcal{M}_{\delta}} p(a | s) da \leq \text{Vol}(\mathcal{M}_{\delta}) \cdot \text{ess sup}_{a \in \mathcal{M}_{\delta}} p(a | s).$$

Applying Lemma 22 to the compact  $C^1$   $k$ -submanifold  $\mathcal{M} \subset \mathbb{R}^d$  provides constants  $C_{\mathcal{M}} > 0$  and  $\bar{\delta} > 0$  such that for all  $0 < \delta \leq \bar{\delta}$ ,

$$\text{Vol}(\mathcal{M}_{\delta}) \leq C_{\mathcal{M}} \delta^{d-k}.$$

Combining the above yields

$$S_{\theta}(s; \delta) \leq C_{\mathcal{M}} \delta^{d-k} \cdot \text{ess sup}_{a \in \mathcal{M}_{\delta}} p(a | s),$$

and therefore

$$H_{\theta}(s; \delta) = 1 - S_{\theta}(s; \delta) \geq 1 - C_{\mathcal{M}} \delta^{d-k} \cdot \text{ess sup}_{a \in \mathcal{M}_{\delta}} p(a | s).$$

Finally, if  $H_{\theta}(s; \delta) \leq \eta$ , then  $S_{\theta}(s; \delta) \geq 1 - \eta$ , and rearranging the success bound gives

$$\text{ess sup}_{a \in \mathcal{M}_{\delta}} p(a | s) \geq \frac{1 - \eta}{C_{\mathcal{M}}} \delta^{-(d-k)}.$$

■

### B. Proof of Generative Trilemma (Theorem 15)

**Theorem 15** (The Precision Trilemma: Collapse, Fold, or Hallucinate). *Let the action be generated by  $a = F(z)$  where  $Z \sim p_Z$ . Assume  $F$  is  $C^1$  on an open set  $U \subseteq \mathcal{Z}$  containing the support of  $p_Z$ , with bounded latent density  $\rho_Z(z) \leq \rho_Z^{\max}$ . Define the active latent set as  $Z_{\delta} := F^{-1}(\mathcal{M}_{\delta}) \cap U$ . Define local folding and local conditioning restricted to this active set:  $N_{\delta} := \text{ess sup}_{a \in \mathcal{M}_{\delta}} \#\{z \in Z_{\delta} : F(z) = a\}$ , and  $\sigma_{*}(\delta) := \text{ess inf}_{z \in Z_{\delta}} \sigma_{\min}(J_F(z))$ , where  $J_F(z)$  is the Jacobian of  $F$  and  $\sigma_{\min}(J_F(z))$  its smallest singular value. Assume  $F$  is finite-to-one on  $Z_{\delta}$  (i.e.,  $N_{\delta} < \infty$ ) and  $\sigma_{*}(\delta) > 0$ . Then the induced action distribution admits a density on  $\mathcal{M}_{\delta}$  and the hallucination rate satisfies*

$$H_{\theta}(s; \delta) \geq 1 - C_{\mathcal{M}} \delta^{d-k} N_{\delta} \rho_Z^{\max} \sigma_{*}(\delta)^{-d}. \quad (3)$$

In particular, if the policy achieves a target hallucination level  $H_{\theta}(s; \delta) \leq \eta$  for some  $\eta \in (0, 1)$ , then the generator must satisfy the following lower bound locally on the tube:

$$\underbrace{N_{\delta}}_{\text{Fold}} \cdot \underbrace{\sigma_{*}(\delta)^{-d}}_{\text{Collapse}} \geq \frac{1 - \eta}{C_{\mathcal{M}} \rho_Z^{\max}} \delta^{-(d-k)}. \quad (4)$$

Hence, as precision tightens ( $\delta \rightarrow 0$ ), any policy that maintains  $H_{\theta}(s; \delta) \leq \eta$  must either fold space ( $N_{\delta} \rightarrow \infty$ ) or collapse volume locally ( $\sigma_{*}(\delta) \rightarrow 0$ ).

*Proof:* Consider the active set  $Z_{\delta} = F^{-1}(\mathcal{M}_{\delta}) \cap U$ . Since  $\sigma_{\min}(J_F(z)) \geq \sigma_{*}(\delta) > 0$  for all  $z \in Z_{\delta}$ , the Inverse Function Theorem implies that  $F$  is a local diffeomorphism in a neighborhood of any point in  $Z_{\delta}$ . Since  $\text{supp}(p_Z) \subseteq U$ , the density of the pushforward distribution  $a = F(z)$  is fully determined by preimages in  $U$ . Using the Area Formula (change-of-variables for many-to-one maps), for almost every  $a \in \mathcal{M}_{\delta}$ :

$$p(a | s) = \sum_{z \in F^{-1}(a) \cap U} \rho_Z(z) |\det J_F(z)|^{-1}.$$

If  $a \in \mathcal{M}_{\delta}$ , then any preimage  $z \in F^{-1}(a) \cap U$  lies in  $Z_{\delta}$  by definition. We bound the terms uniformly: itemsep=1pt,topsep=1pt

- 1) Density:  $\rho_Z(z) \leq \rho_Z^{\max}$ .

2) Jacobian: for  $z \in Z_\delta$ ,  $|\det J_F(z)| \geq (\sigma_{\min}(J_F(z)))^d \geq \sigma_*(\delta)^d$ .

Substituting these bounds into the sum gives, for a.e.  $a \in \mathcal{M}_\delta$ ,

$$\begin{aligned} p(a \mid s) &\leq \sum_{z \in F^{-1}(a) \cap U} \frac{\rho_Z^{\max}}{\sigma_*(\delta)^d} \\ &= \#\{z \in Z_\delta : F(z) = a\} \cdot \rho_Z^{\max} \cdot \sigma_*(\delta)^{-d}. \end{aligned}$$

Taking the essential supremum over  $a \in \mathcal{M}_\delta$  yields

$$\text{ess sup}_{a \in \mathcal{M}_\delta} p(a \mid s) \leq N_\delta \rho_Z^{\max} \sigma_*(\delta)^{-d}.$$

Applying Lemma 14,

$$H_\theta(s; \delta) \geq 1 - C_{\mathcal{M}} \delta^{d-k} \cdot \text{ess sup}_{a \in \mathcal{M}_\delta} p(a \mid s),$$

and substituting the bound on  $\text{ess sup}_{\mathcal{M}_\delta} p$  proves (3). Finally, if  $H_\theta(s; \delta) \leq \eta$ , then the lower bound (3) must not exceed  $\eta$ , i.e.,

$$1 - C_{\mathcal{M}} \delta^{d-k} N_\delta \rho_Z^{\max} \sigma_*(\delta)^{-d} \leq \eta,$$

which we can rearrange to (4).  $\blacksquare$

### C. Proof of K-step tradeoff (Corollary 16)

**Corollary 16** (K-step precision tradeoff). *Assume the decoder is a K-step composition  $F^{(K)} = \Phi_{K-1} \circ \dots \circ \Phi_0$ , where each  $\Phi_t$  is a  $C^1$  diffeomorphism and there exist constants  $\lambda_t > 0$  such that  $\sigma_{\min}(J\Phi_t(z)) \geq \lambda_t$  for all  $z$ . Then the overall map is one-to-one (no folding) and  $\sigma_*(\delta) \geq \inf_{z \in Z_\delta} \sigma_{\min}(JF^{(K)}(z)) \geq \prod_{t=0}^{K-1} \lambda_t$ . Then, for all  $0 < \delta \leq \bar{\delta}$ ,*

$$H_\theta^{(K)}(s; \delta) \geq 1 - C_{\mathcal{M}} \rho_Z^{\max} \left( \prod_{t=0}^{K-1} \lambda_t \right)^{-d} \delta^{d-k}.$$

In particular, if  $\lambda_t \geq \lambda \in (0, 1]$  for all  $t$ , then  $H_\theta^{(K)}(s; \delta) \geq 1 - C_{\mathcal{M}} \rho_Z^{\max} \lambda^{-dK} \delta^{d-k}$ . A necessary condition to bound the hallucination rate  $H_\theta^{(K)}(s; \delta) \leq \eta \in (0, 1)$  is

$$K \geq \frac{1}{d \log(1/\lambda)} \left[ (d-k) \log \frac{1}{\delta} + \log \frac{1-\eta}{C_{\mathcal{M}} \rho_Z^{\max}} \right]. \quad (5)$$

Note: the bound is vacuous when the right-hand side is negative.

*Proof:* Since each  $\Phi_t$  is a diffeomorphism, their composition  $F^{(K)}$  is a diffeomorphism, hence  $N_\delta = 1$ . The singular-value lower bound follows from the chain rule and the standard inequality  $\sigma_{\min}(AB) \geq \sigma_{\min}(A)\sigma_{\min}(B)$ . Apply Theorem 15 with  $N_\delta = 1$  and  $\sigma_*(\delta) \geq \prod_t \lambda_t$  to obtain the hallucination bound. Rearranging and taking logs gives the number of required steps in (5).  $\blacksquare$

## APPENDIX C PLANNING HALLUCINATIONS: PROOFS AND ADDITIONAL DETAILS

### A. Proof for Horizon Barrier (Lemma 17)

**Lemma 17** (Horizon Barrier). *Let  $(S_t)_{t=0}^T$  be the rollout from  $s_0$ . Define  $p_t(s) := \Pr_{Z \sim p_Z} [\pi_\theta(s, Z) \in \mathcal{A}_{\text{prog}}(s, t)]$  and  $\gamma_t := \sup_{s \in \Sigma_t} p_t(s)$ . Then the rollout success probability factorizes and is upper bounded by*

$$H_{\pi_\theta}^{\text{plan}}(I) \geq 1 - \prod_{t=1}^T \gamma_t.$$

In particular, if  $\gamma_t \leq \gamma < 1$  for all  $t$ , then  $\Pr[f_{\text{plan}}(s_0, \tau_\theta) = 1] \leq \gamma^T$  and  $H_{\pi_\theta}^{\text{plan}}(I) \geq 1 - \gamma^T$ .

*Proof:* Let  $E_k := \{\pi_\theta(S_k, Z_k) \in \mathcal{A}_{\text{prog}}(S_k, T-k)\}$  for  $k = 0, \dots, T-1$ . Under deterministic dynamics and the definition of  $\mathcal{A}_{\text{prog}}$ , the plan is valid if and only if  $\bigcap_{k=0}^{T-1} E_k$  occurs. By the chain rule,

$$\Pr \left[ \bigcap_{k=0}^{T-1} E_k \right] = \prod_{k=0}^{T-1} \Pr[E_k \mid E_0 \cap \dots \cap E_{k-1}] = \prod_{t=1}^T \gamma_t,$$

where we re-indexed with  $t = T - k$ .

On the event  $E_0 \cap \dots \cap E_{T-t-1}$ , the rollout state  $S_{T-t}$  must lie in  $\Sigma_t$  by definition of  $\mathcal{A}_{\text{prog}}(S_{T-t-1}, t+1)$  and  $\Sigma_t$ . Therefore  $p_t(S_{T-t}) \leq \sup_{s \in \Sigma_t} p_t(s) = \gamma_t$  pointwise on this event, implying  $\eta_t \leq \gamma_t$ . Hence

$$\Pr[f_{\text{plan}} = 1] = \prod_{t=1}^T \eta_t \leq \prod_{t=1}^T \gamma_t,$$

and the hallucination bounds follow by complement. The  $\gamma^T$  specialization is immediate when  $\gamma_t \leq \gamma$  for all  $t$ .  $\blacksquare$

### B. Proof for Reliability search budget window

**Lemma 20** (Reliability search-budget window). *Consider any verification-guided planner with budget  $q$  and verifier error rates  $(\varepsilon_{\text{fp}}, \varepsilon_{\text{fn}})$ , and let  $c := 1 - \varepsilon_{\text{fn}}$ . Let  $(\rho_j)_{j=1}^q$  be its amplification schedule (Definition 19). Then*

$$\begin{aligned} H(I) &\leq \varepsilon_{\text{fp}} \sum_{j=1}^q \Pr[C_{j-1}] (1 - \rho_j) \leq q \varepsilon_{\text{fp}} \\ A(I) &\leq \prod_{j=1}^q (1 - c \rho_j). \end{aligned}$$

Consequently, the planner is certified to be  $(\alpha, \beta)$ -reliable whenever  $q \varepsilon_{\text{fp}} \leq \alpha$  and  $\prod_{j=1}^q (1 - c \rho_j) \leq \beta$ .

*Proof:* **Hallucination bound.** Let  $\mathcal{F}_{j-1}$  denote the  $\sigma$ -field generated by the planner's history up to round  $j-1$  (including past sampled indices and verifier outcomes). Conditional on  $\mathcal{F}_{j-1}$  and  $C_{j-1}$ , the planner samples  $J_j \sim Q_j$ , where  $Q_j$  is  $\mathcal{F}_{j-1}$ -measurable. Let  $F_j$  be the event of a false acceptance at round  $j$ :

$$F_j := \{C_{j-1} \wedge J_j \notin V \wedge \tilde{f}_{\text{plan}}(s_0, \tau^{J_j}) = 1\}.$$

If the planner hallucinates, then some  $F_j$  occurs, hence

$$\{\hat{\tau} \neq \perp \wedge f_{\text{plan}}(s_0, \hat{\tau}) = 0\} \subseteq \bigcup_{j=1}^q F_j,$$

and

$$H(I) = \sum_{j=1}^q \Pr[F_j].$$

By the false-positive guarantee, for every invalid index  $i \notin V$  and every round  $j$ ,

$$\Pr[\tilde{f}_{\text{plan}}(s_0, \tau^i) = 1 \mid \mathcal{F}_{j-1}, J_j = i] \leq \varepsilon_{\text{fp}}.$$

Therefore, conditioning on  $\mathcal{F}_{j-1}$ ,

$$\begin{aligned} \Pr[F_j \mid \mathcal{F}_{j-1}] &= \mathbf{1}\{C_{j-1}\} \sum_{i \notin V} Q_j(i) \Pr[\tilde{f}_{\text{plan}}(s_0, \tau^i) = 1 \mid \mathcal{F}_{j-1}, J_j = i] \\ &\leq \mathbf{1}\{C_{j-1}\} \varepsilon_{\text{fp}} \sum_{i \notin V} Q_j(i) \\ &= \mathbf{1}\{C_{j-1}\} \varepsilon_{\text{fp}} (1 - Q_j(V)). \end{aligned}$$

Taking expectations and using the tower property gives

$$\Pr[F_j] = \mathbb{E}[\Pr[F_j \mid \mathcal{F}_{j-1}]] \leq \varepsilon_{\text{fp}} \mathbb{E}[\mathbf{1}\{C_{j-1}\} (1 - Q_j(V))].$$

Now define

$$\rho_j := \Pr[J_j \in V \mid C_{j-1}] = \mathbb{E}[Q_j(V) \mid C_{j-1}],$$

so that

$$\mathbb{E}[\mathbf{1}\{C_{j-1}\} (1 - Q_j(V))] = \Pr[C_{j-1}] (1 - \rho_j).$$

Hence

$$\Pr[F_j] \leq \varepsilon_{\text{fp}} \Pr[C_{j-1}] (1 - \rho_j),$$

and

$$H(I) \leq \varepsilon_{\text{fp}} \sum_{j=1}^q \Pr[C_{j-1}] (1 - \rho_j) \leq q \varepsilon_{\text{fp}}.$$

**Abstention bound.** Let  $C_j$  denote the event that the planner reaches round  $j + 1$  (no acceptance in rounds  $1, \dots, j$ ). Then  $A(I) = \Pr[C_q]$  and by the chain rule

$$\Pr[C_q] = \prod_{j=1}^q \Pr[C_j \mid C_{j-1}], \quad C_0 \text{ is the sure event.}$$

Fix round  $j$  and condition on  $C_{j-1}$ . A *true acceptance* occurs if  $J_j \in V$  and the verifier does not commit a false negative. Since  $\Pr[J_j \in V \mid C_{j-1}] = \rho_j$  and valid plans are accepted with probability at least  $c$ ,

$$\Pr[\text{true accept at round } j \mid C_{j-1}] \geq c \rho_j.$$

Therefore, the probability of *no acceptance* at round  $j$  is at most  $1 - c \rho_j$ :

$$\Pr[C_j \mid C_{j-1}] \leq 1 - c \rho_j.$$

Multiplying over  $j$  yields  $A(I) = \Pr[C_q] \leq \prod_{j=1}^q (1 - c \rho_j)$ . The certification conditions follow by enforcing the two upper bounds to be at most  $(\alpha, \beta)$ .  $\blacksquare$

### C. Non-adaptive proposal-and-verify window and horizon fragility

Lemma 20 is a useful tool to study how fast this adaptation must take place. The corollaries below and in the main text specialize the lemma to specific conditional mass schedules to see if they can overcome the horizon barrier. Below, we show the case of a common non-adaptive planner.

**Corollary 23** (Non-adaptive proposal-and-verify window and horizon fragility). *Assume  $Q_j \equiv Q$  (no adaptation), and let  $\rho := Q(V)$  and  $c := 1 - \varepsilon_{\text{fn}}$ . Then, the planner is certified to be  $(\alpha, \beta)$ -reliable whenever there exists an integer  $q$  satisfying*

$$q \leq \frac{\alpha}{\varepsilon_{\text{fp}}} \quad \text{and} \quad (1 - c \rho)^q \leq \beta,$$

i.e.,

$$\frac{\log \beta}{\log(1 - c \rho)} \leq q \leq \frac{\alpha}{\varepsilon_{\text{fp}}}.$$

Moreover, if the proposal  $Q$  is induced by rolling out a  $T$ -step sequential policy and the horizon barrier yields

$$\rho = \Pr_{\tau \sim Q} [f_{\text{plan}}(s_0, \tau) = 1] \leq \gamma^T \quad \text{for some } \gamma \in (0, 1),$$

then (for small  $c \gamma^T$ ) the abstention constraint requires

$$q \gtrsim \frac{1}{c \gamma^T} \log\left(\frac{1}{\beta}\right),$$

which is exponential in  $T$ .

*Proof:* If  $Q_j \equiv Q$ , then  $\rho_j = \Pr[J_j \in V \mid C_{j-1}] = Q(V) = \rho$  for all  $j$ . The bounds  $H(I) \leq q \varepsilon_{\text{fp}}$  and  $A(I) \leq (1 - c \rho)^q$  follow from Lemma 20. Taking logs yields the explicit window. For the final statement, substitute  $\rho \leq \gamma^T$ . Using  $-\log(1-x) \approx x$  for small  $x$  gives the approximation  $q \gtrsim \log(1/\beta)/(c \gamma^T)$ , exhibiting the exponential-in- $T$  scaling.  $\blacksquare$

Corollary 23 formalizes why non-adaptive propose-and-verify planners are fragile at long horizons. If the proposal distribution is induced by rolling out a sequential policy, the horizon barrier suggests  $\rho_1$  can be as small as  $\gamma^T$ , making the number of independent tries needed to avoid abstention exponential in  $T$ —often far beyond the safe search budget afforded by  $\varepsilon_{\text{fp}}$ . If the verifier is too noisy or the plan proposal  $Q$  is too poor, the feasibility window can simply close and *no* amount of test-time compute can salvage the system.

### D. Cumulative valid-mass condition for abstention control (Corollary 24)

**Corollary 24** (Cumulative valid-mass condition for abstention control). *Under the assumptions of Lemma 20,  $A(I) \leq \exp\left(-c \sum_{j=1}^q \rho_j\right)$ . Therefore, a sufficient condition for  $A(I) \leq \beta$  is  $\sum_{j=1}^q \rho_j \geq \frac{1}{c} \log\left(\frac{1}{\beta}\right)$ .*

*Proof:* From Lemma 20,  $A(I) \leq \prod_{j=1}^q (1 - c \rho_j)$ . Apply  $1 - x \leq e^{-x}$  with  $x = c \rho_j$  and multiply:

$$\prod_{j=1}^q (1 - c \rho_j) \leq \prod_{j=1}^q e^{-c \rho_j} = e^{-c \sum_{j=1}^q \rho_j}.$$

Rearrange  $e^{-c \sum \rho_j} \leq \beta$  to obtain  $\sum \rho_j \geq (1/c) \log(1/\beta)$ .  $\blacksquare$

### E. Proof for Amplification-rate to beat the horizon barrier (Theorem 21)

**Theorem 21** (Amplification-rate to beat the horizon barrier). *Consider a verification-guided planner with verifier error rates  $(\varepsilon_{\text{fp}}, \varepsilon_{\text{fn}})$ , amplification schedule  $(\rho_j)_{j=1}^q$  (Definition 19) and targets  $(\alpha, \beta)$ -reliability. Let  $c := 1 - \varepsilon_{\text{fn}}$ . Then, any  $(\alpha, \beta)$ -reliable planner must satisfy  $\sum_{j=1}^q \rho_j \geq 1 - \alpha - \beta$ . Assume the horizon barrier yields an exponentially small initial valid-plan mass  $\rho_1 \leq \gamma^T$  for some  $\gamma \in (0, 1)$ .*

(i) **Polynomial amplification is insufficient.** If  $\rho_j \leq \rho_1 j^p$  for some  $p \geq 0$  and all  $j \leq q$ , then

$$\sum_{j=1}^q \rho_j \leq \rho_1 \sum_{j=1}^q j^p \leq \gamma^T \cdot \frac{(q+1)^{p+1} - 1}{p+1}.$$

Consequently, meeting the necessary condition  $\sum_{j=1}^q \rho_j \geq 1 - \alpha - \beta$  requires

$$q \geq \left(1 + \frac{(p+1)(1 - \alpha - \beta)}{\gamma^T}\right)^{\frac{1}{p+1}} - 1,$$

which is exponential in  $T$  for constant  $\gamma \in (0, 1)$ .

(ii) **Geometric amplification is sufficient** (if within the verifier budget). If  $\rho_j \geq \rho_1 r^{j-1}$  for all  $j \leq q$  for some  $r > 1$ , then

$$\sum_{j=1}^q \rho_j \geq \rho_1 \sum_{j=1}^q r^{j-1} = \rho_1 \cdot \frac{r^q - 1}{r - 1}.$$

In particular, a sufficient condition for  $(\alpha, \beta)$ -reliability is

$$q \varepsilon_{\text{fp}} \leq \alpha \quad \text{and} \quad \rho_1 \cdot \frac{r^q - 1}{r - 1} \geq \frac{1}{c} \log\left(\frac{1}{\beta}\right).$$

Hence, geometric amplification requires  $q = \Theta(\log(1/\rho_1))$ . In regimes where  $\rho_1 \approx \gamma^T$  (as suggested by the rollout factorization), this gives  $q = \Theta(T)$ .

*Proof:* Let  $E_{\text{val}} := \{\hat{\tau} \neq \perp \wedge f_{\text{plan}}(s_0, \hat{\tau}) = 1\}$ , so that  $S(I) = \Pr[E_{\text{val}}]$ . If the planner outputs a valid plan, then some round must have proposed a valid index:

$$E_{\text{val}} \subseteq \bigcup_{j=1}^q \{J_j \in V\}.$$

Hence  $S(I) \leq \sum_{j=1}^q \Pr[J_j \in V]$  by a union bound. Also,  $\Pr[J_j \in V] = \Pr[C_{j-1}] \Pr[J_j \in V \mid C_{j-1}] = \Pr[C_{j-1}] \rho_j \leq \rho_j$ . Therefore  $S(I) \leq \sum_{j=1}^q \rho_j$ . If the planner is  $(\alpha, \beta)$ -reliable, then  $S(I) = 1 - A(I) - H(I) \geq 1 - \alpha - \beta$ , implying

$$\sum_{j=1}^q \rho_j \geq 1 - \alpha - \beta. \tag{7}$$

(i) is immediate by substituting the polynomial upper bound on  $\rho_j$  and using  $\sum_{j=1}^q j^p \leq \int_0^q (x+1)^p dx = \frac{(q+1)^{p+1} - 1}{p+1}$ , then enforcing (7).

(ii) follows from the geometric-series lower bound on  $\sum_{j=1}^q \rho_j$  and applying Lemma 20 and Corollary 24 to certify  $H(I) \leq \alpha$  and  $A(I) \leq \beta$ . ■

### F. Action Chunking and the Barriers

A common intuition is that if the primitive action is very low-level (e.g., small joint deltas), then the safe set  $\mathcal{A}_{\text{safe}}(s) = \{a : f_{\text{phys}}(s, a) = 1\}$  is often connected in many states, seemingly avoiding the topological barrier from Section IV-A. This is frequently true at the *one-step* level, but it does *not* remove multimodality for long-horizon goal-reaching. Chunking trades *fewer decisions* against a *harder per-decision sampling problem*: `leftmargin=*,itemsep=2pt,topsep=2pt`

- 1) *Topology reappears at the progress/chunk level.* Even if  $\mathcal{A}_{\text{safe}}(s)$  is connected for small one-step controls, the *progress* set  $\mathcal{A}_{\text{prog}}(s, t)$  can be disconnected at reachability bottlenecks. Two small safe actions can lead into different time-bounded reachable basins  $\Sigma_{t-1}$ , while “in-between” actions can be safe but *non-progress* (leading to dead ends or timeouts). Chunking amplifies this effect since the progress set typically decomposes into more separated components (distinct partial trajectories/contact-mode prefixes), activating the same “seam” phenomenon from Section IV-A, now with respect to progress/plan validity rather than one-step physical invalidity.

- 2) *Precision compounds within a chunk.* In contact-rich tasks (Section IV-B), progress may require staying in a thin tube (or near a manifold) over multiple successive steps. Requiring consecutive steps in the chunk to remain in such a tube makes the feasible region effectively thinner, decreasing the per-sample mass of  $\mathcal{A}_{\text{prog}}(s, t)$  (often sharply) as the chunk length grows.
- 3) *Horizon compounding improves in count, worsens in mass.* If the policy outputs chunks of length  $\ell$  and commits to executing them, then Lemma 17 applies with an *effective* horizon of roughly  $\lceil T/\ell \rceil$ . Increasing  $\ell$  reduces the number of factors in this product (helping the horizon barrier) but typically decreases each factor  $\gamma_t$  (harder chunk feasibility due to topology/precision and open-loop drift), creating a natural “sweet spot” in  $\ell$ .

This view also clarifies a common empirical design; predict long chunks for temporal coherence but execute only a short prefix before replanning (receding-horizon), which reduces open-loop compounding and delays irreversible mode commitment while still leveraging temporally structured proposals.

## APPENDIX D EXPERIMENTAL SETUP

### A. Topology Barrier

This appendix describes the implementation and hyperparameters used for the 2D band topology experiments in which we measure action hallucination and relate it to the isoperimetric lower bound.

**Band action-space geometry and safe modes.** Actions are two-dimensional,  $a = (x, y) \in \mathbb{R}^2$ , with an *action band*

$$x \in [x_{\min}, x_{\max}], \quad y \in [-y_{\max}, y_{\max}].$$

Within this band, the safe set is the union of  $M$  disconnected horizontal strips  $\{U_i\}_{i=1}^M$  separated by forbidden gaps. Let  $r$  denote the strip half-width (`strip_halfwidth`) and  $W$  denote the gap half-width. The strip centers are placed symmetrically about 0 with spacing  $2(r + W)$ , i.e.

$$\mu_i = \left(i - \frac{M-1}{2}\right) 2(r + W), \quad i \in \{0, \dots, M-1\}.$$

The safe strips are

$$U_i = \{(x, y) : x \in [x_{\min}, x_{\max}], y \in [\mu_i - r, \mu_i + r]\}.$$

Any action outside the band, or in the gaps between strips, is forbidden and counted as a hallucination.

**Training data distribution.** We train on i.i.d. safe actions sampled from the union of strips. In the experiments reported here, we perform the following:

- sample mode index  $i \sim \text{Categorical}(\pi)$  with  $\pi$  uniform over modes,
- sample  $x \sim \text{Uniform}[x_{\min}, x_{\max}]$ ,
- sample  $y \sim \text{Uniform}[\mu_i - r, \mu_i + r]$ .

**Models.** All methods produce actions deterministically from a latent/noise variable in  $\mathbb{R}^2$ ; throughout, the base latent distribution is  $Z \sim \mathcal{N}(0, I_2)$ . We implemented two models:

- **Flow Matching.** We train a rectified flow vector field  $v_\theta(x, t)$  with  $t \in [0, 1]$  using flow-matching:

$$x_t = (1-t)x_0 + tx_1, \quad x_0 \sim p_{\text{data}}, \quad x_1 \sim \mathcal{N}(0, I_2),$$

with target velocity  $v^*(x_t, t) = x_1 - x_0$ , optimized via MSE  $\|v_\theta(x_t, t) - v^*(x_t, t)\|_2^2$ . Sampling is deterministic Euler (or Heun) integration from  $t = 1$  to  $t = 0$  starting at Gaussian noise.

- **Diffusion.** We train a v-pred diffusion model with cosine schedule (default  $T = 200$ ) and exponential moving average (EMA) of parameters. Training uses MSE on the  $v$ -prediction target. Sampling is deterministic DDIM (i.e.  $\eta = 0$ ) with a user-specified number of sampling steps.

Both the flow and diffusion networks use the same backbone: a sinusoidal time embedding of dimension 64, concatenated with the 2D input, followed by an MLP with `depth=4` hidden layers of width `hidden=256`, with `LayerNorm` and `SiLU` activations, and a final linear layer to  $\mathbb{R}^2$ . We optimize with AdamW (default learning rate  $2 \times 10^{-4}$ , weight decay  $10^{-4}$ ), batch size 2048, and gradient-norm clipping at 1.0. Unless otherwise stated, we train each model for 100,000 steps.

**Evaluation protocol and metrics.** For each configuration (defined by  $(M, W)$  and the “smoothness” settings), and for each random seed, we generate  $N = 10^6$  samples in batches of 4096. For each method we compute the (i) Hallucination probability,  $H = \Pr[a(Z) \notin \bigcup_{i=1}^M U_i]$ , where any sample outside the band or in the gaps counts as forbidden, and (ii) the mode masses:  $p_i = \Pr[a(Z) \in U_i]$  for  $i \in \{1, \dots, M\}$ . We estimate a distribution of local Lipschitz proxies on the typical latent ball  $B_R = \{z : \|z\| \leq R\}$  with  $R = 3.0$  by sampling 2048 points from  $Z \sim \mathcal{N}(0, I_2)$  truncated to  $B_R$ , and estimating  $\sigma_{\max}(z) \approx \|J(z)\|_{\text{op}}$  via finite differences with step size 0.01.

## B. Precision Barrier

We study a controlled “glass/mug grasp” proxy in which valid actions lie on a low-dimensional manifold  $\mathcal{M} \subset \mathbb{R}^d$ . Similar to the topological experiments, we train two generative models (Flow Matching and Diffusion, as in the topology experiments) on the same synthetic manifold distribution and compare them under consistent evaluation. Each action is represented by a 7D vector

$$a = [x, y, h, \text{roll}, \text{pitch}, \sin(\text{yaw}), \cos(\text{yaw})] \in \mathbb{R}^7, \quad (8)$$

where yaw is encoded as  $(\sin, \cos)$  to avoid discontinuities at  $\pm\pi$ . Coordinates are normalized so that a Euclidean distance meaningfully mixes translational and rotational components.

**Ideal side-grasp manifold.** The ideal grasp manifold  $\mathcal{M}$  is parameterized by two intrinsic coordinates:

- $\theta \in [0, 2\pi]$ : angle around the mug,
- $h$  in a valid height interval  $[h_{\min}, h_{\max}]$ .

This defines a  $k = 2$  dimensional manifold embedded in an ambient space of dimension  $d = 7$ , hence codimension  $d - k = 5$ . Points on  $\mathcal{M}$  satisfy: (i)  $(x, y)$  lies on a ring of fixed radius  $r$  (mug radius plus clearance), (ii) roll and pitch are zero, (iii) yaw points inward toward the mug center (a deterministic function of  $\theta$ ), and (iv)  $h$  lies in  $[h_{\min}, h_{\max}]$ . For any  $a \in \mathbb{R}^7$ , we compute

$$\text{dist}(a, \mathcal{M}) := \|a - \Pi_{\mathcal{M}}(a)\|_2, \quad (9)$$

where  $\Pi_{\mathcal{M}}$  is an analytic projection that solves for the best  $\theta^*$  (by jointly aligning the  $(x, y)$  ring constraint and yaw  $(\sin, \cos)$  consistency), clamps  $h$  to  $[h_{\min}, h_{\max}]$ , and sets roll/pitch to 0.

**Evaluation protocol and metrics.** For a trained model, we generate i.i.d. samples  $\{x^{(i)}\}_{i=1}^N$  and evaluate the action hallucination curve

$$H(\delta) = \mathbb{P}(\text{dist}(x, \mathcal{M}) > \delta) \approx \frac{1}{N} \sum_{i=1}^N \mathbf{1}[\text{dist}(x^{(i)}, \mathcal{M}) > \delta], \quad (10)$$

over a log-spaced grid  $\delta \in [\delta_{\min}, \delta_{\max}]$ . To probe whether concentration near a lower-dimensional manifold requires ill-conditioned transformations, we analyze Jacobians of sampler maps. Let a sampler consist of step maps  $x_{k+1} = F_k(x_k)$ , for  $k = 0, \dots, K - 1$ , so the overall map is  $G = F_{K-1} \circ \dots \circ F_0$ . We compute per-step Jacobians  $J_k = \partial F_k / \partial x$  and the global Jacobian

$$J_{\text{global}} = \frac{\partial G}{\partial x} = J_{K-1} \cdots J_0. \quad (11)$$

Conditioning is summarized via singular values  $\sigma_{\min}(J)$  and diagnostics are computed along random sampler trajectories initialized from Gaussian noise.

## AUTHOR CONTRIBUTIONS AND LLM USAGE

H. Soh conceived the central idea and wrote the majority of the manuscript. E. Lim verified the proofs and contributed improvements to the technical statements. Large language models were used to assist with idea exploration, proof development, code implementation, and manuscript editing. Illustrative images depicting the robot in various environments were generated using Gemini, while all schematic figures were created by H. Soh. All plots were produced from experiments described in the paper and appendix. The authors take full responsibility for the content of this work.